Technical Report
TR-17-03
February 2018

Numerical modelling of the buffer swelling test in Äspö HRL

Validation of numerical models with the buffer swelling test data

Martino Leoni
Lennart Börgesson
Paula Keto

SVENSK KÄRNBRÄNSLEHANTERING AB

SWEDISH NUCLEAR FUEL
AND WASTE MANAGEMENT CO

Box 3091, SE-169 03 Solna
Phone +46 8 459 84 00
skb.se

SVENSK KÄRNBRÄNSLEHANTERING

ISSN 1404-0344
SKB TR-17-03
ID 1525659
February 2018

Numerical modelling of the buffer swelling test in Äspö HRL

Validation of numerical models with the buffer swelling test data

Martino Leoni, Wesi Geotecnica Srl

Lennart Börgesson, Clay Technology AB

Paula Keto, B+Tech Oy

Keywords: Bentonite, Backfill, Modelling, Field test, FEM, Blocks, Cracks, Abaqus, PLAXIS, Äspö HRL, KBP1012.

Abstract

This report describes the numerical modelling of the Buffer swelling test performed in Äspö HRL. The field test was used to simulate the heave of saturated buffer to dry backfill consisting of a thin ~ 10 cm thick bentonite pellet bed, backfill blocks placed on the top of the bed and pellets placed around the blocks. The swelling of the buffer in a deposition hole was simulated with hydraulic jacks pushing a steel plate towards the backfill with stepwise increase of the pressure. In the test at Äspö HRL, this resulted in compression of the pellet bed, uplift and compression of the block masonry and breakage of some of the backfill blocks placed above the deposition hole.

Two different modelling approaches were used to model the filed test. The finite element codes Abaqus and PLAXIS were used in the calculations. Despite some differences between the codes used, material models, geometry and input data, both approaches were able to predict the behaviour until diffused failure of the blocks occurred. As a conclusion both codes and models can be used for studying the processes in a dry backfill of pellets and blocks when the buffer swells towards the backfill, within their scope of applicability.

The field test showed that the backfill reached its maximum resistance against buffer swelling when the simulated buffer swelling pressure increased close to the uniaxial compression strength of the individual blocks. If confirmed for a wider range of block strengths, this should be taken into account in further development of the backfill concept.

Sammanfattning

Rapporten beskriver numerisk modellering av buffertuppsvällningsförsöket i Äspö HRL. Försöket simulerade hävningen av en vattenmättad buffert mot en tunnelåterfyllning som bestod av en 10 cm tjock bentonitebädd av pellets med återfyllningsblock placerade ovanpå pelletsbädden och pellets placerade i spalterna mellan blocken och berget. Buffertens svällning i deponerinsghålet simulerades med hydrauliska domkrafter som tryckte en stålplatta placerad under pelletsbädden mot återfyllningen genom att stegvis öka trycket. Resultatet av försöket blev en kompression av pelletsbädden, upptryckning och kompression av blockfyllningen och bräckage av en del block placerade ovanför det simulerade deponeringshålet.

Två modelleringstekniker användes för att modellera fältförsöket. Finita elementkoderna Abaqus och PLAXIS användes för beräkningarna. Trots skillnaderna mellan de använda koderna och skillnader i materialmodeller, geometrier och indata lyckades båda teknikerna modellera händelseförloppet fram till dess att blocken började gå sönder. En slutsats är att båda koderna och modellerna kan användas för att studera processerna i återfyllningen när bufferten sväller upp mot en torr återfyllning av block och pellets.

Fältförsöket visade att återfyllningen uppnår sitt maximala motstånd mot buffertuppsvällning när svälltrycket från bufferten är nära den enaxliga tryckhållfastheten hos de individuella blocken. Om detta kan bekräftas för ett vidare spann av tryckhållfastheter bör det beaktas vid den forsatta utvecklingen av återfyllningskonceptet.

Foreword

This report is part of Posiva and SKB cooperation on computational modelling of swelling of the wet buffer into the dry backfill. The content of the report is based on the modelling work done by Lennart Börgesson (Clay Technology AB), Jan Hernelind (5T Engineering AB) and by Martino Leoni (Wesi Geotecnica Srl). The field test used for model validation, the Buffer swelling test, is a field test by SKB performed in Äspö HRL and reported in Sandén et al. (2017). The work by SKB has been coordinated by Peter Eriksson and the work by Posiva by Kari Koskinen. Both of them have also been reviewing of this report. Paula Keto (B+Tech Oy) has taken part in coordination of the project, writing Chapter 1 of this report and working as technical editor and as a link to the backfill design development work. Xavier Pintado (B+Tech Oy) has taken in part in steering of the work and has reviewed the report. The official reviewers of this report are Jordi Alcoverro (UPC), Patrik Sellin (SKB) and Esther Johnsson (SKB). The authors of the report would like to thank SKB and Posiva on the possibility to take part in this work, SKB for organizing the Buffer swelling test and the reviewers for fruitful comments. In the end we would like to thank all the people taking part in this work for pleasant cooperation.

Contents

1 Introduction

1.1 Background

In both Sweden and Finland, the repository for the spent nuclear fuel is based on the KBS-3V concept. In a repository utilizing the KBS-3V method, each canister containing spent nuclear fuel is placed vertically into a hole drilled in the floor of deposition tunnels as shown in Figure 1-1. The canister is surrounded by highly compacted bentonite clay (buffer). In the deposition tunnels above the deposition holes backfill is used to fill the excavation. The backfill consists of pre-compacted backfill blocks, foundation layer material (bentonite pellets or in situ compacted bentonite) and pellet fill between the blocks and the rock.

Both buffer and backfill are considered as engineered barriers together with the spent nuclear fuel matrix and the canister and other closing structures providing the primary containment against the release of radionuclides. The host rock is considered as a natural barrier providing favourable conditions for the long-term performance of the engineered barriers, but has also the function to limit or retard the transport of radionuclides. Together the engineered barriers and the host rock constitute a multi-barrier system. According to the (Finnish law) Government Decree GD 736/2008: "*The long-term safety of disposal shall be based on safety functions achieved through mutually complementary barriers so that a deficiency of an individual safety function or a predictable geological change will not jeopardise the long-term safety.*"

Considering the roles of the backfill in the multibarrier system, one important safety function of the backfill is to restrict upward buffer swelling/expansion into the overlying deposition tunnel (Posiva 2012). If the buffer can swell upwards it will lose some of its density and by that also important properties required for the buffer, e.g. low hydraulic conductivity and high swelling pressure. An extreme scenario is the so called dry case of buffer/backfill interaction meaning that the water inflow into the deposition tunnel is very low but at the same time there is a fast wetting of a deposition hole. This means that the buffer in the deposition hole will swell and there will be a pressure build up pushing the dry backfill upwards. In order to study this process and its effect on the system performance, numerical modelling has previously been performed of the Swedish deposition tunnel case by Börgesson and Johannesson (2006), Börgesson and Hernelind (2009, 2014) and of the Finnish deposition tunnel case by Leoni (2013). The modelling codes used in the first case has been Abaqus and in the latter case PLAXIS 2D and 3D. Also the material models used have been different.

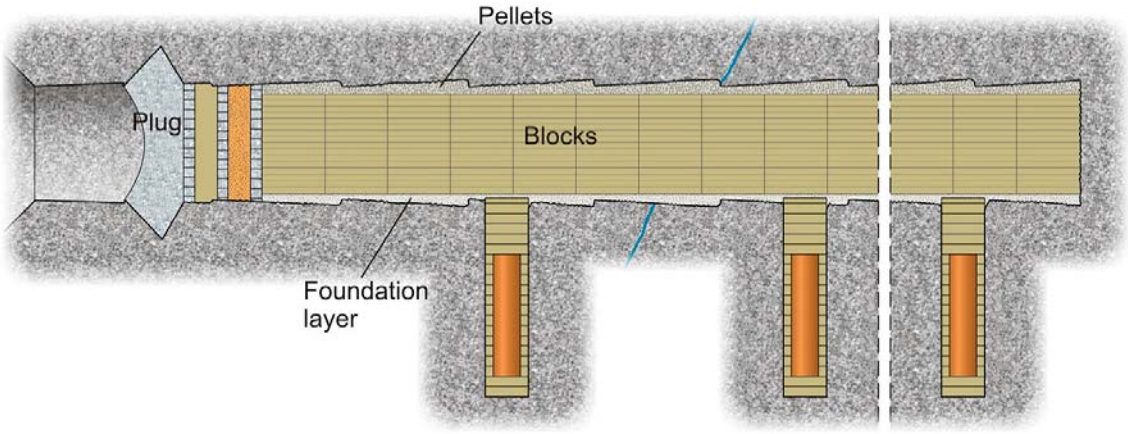

Figure 1-1. *A schematic figure showing a deposition tunnel with vertical deposition holes with spent nuclear fuel canisters and buffer bentonite blocks surrounding them (Keto 2013). The main components of the backfill are pre-compacted backfill blocks, foundation layer and pellet fill.*

In order to study the swelling of the buffer in the dry backfill case, SKB peformed a full-scale field test in Äspö HRL, called the Buffer swelling test (Sandén et al. 2017). In this test the buffer swelling was simulated with a steel plate with an underlying hydraulic jack rising from the buffer hole (see Chapter 2 on the description of the tests). The Buffer swelling test has been used to check and calibrate the calculation technique and the mechanical properties of the backfill block masonry. A sensitivity analysis has also been done in order to see how the properties of the masonry (and especially the joints), the pellet filling and the thickness of the pellet filled slots between the backfill blocks and the rock affect the upwards swelling but this analysis is not reported here. In addition, this test offered the possibility for comparison of the two different modelling approaches used previously by SKB and Posiva. The SKB part of the work including the sensistivity analysis is reported separately in Börgesson and Hernelind (2017).

1.2 Objectives of this report

The objectives of this report are to:

- Present the results from modelling the Buffer swelling test.
- Compare the results gained with the two different modelling approaches.
- Present the results from model validation point of view.

1.3 Limitations

This work is limited to modelling of the Buffer swelling test and model validation. In addition, the modelled case is limited to dry backfill case.

2 Description of the buffer swelling test

An overview of the test and the results is given in this chapter. The text and figures are mainly taken from the Buffer swelling test report (Sandén et al. 2017).

2.1 Test description

A drawing showing the principle test design is provided in Figure 2-1. An “artificial deposition hole” with a depth of about 1.5 meter was drilled in the tunnel floor. A concrete tube with an inner diameter of 1 600 mm was placed in the hole and the slot between the tube and the rock was filled with concrete. Four hydraulic jacks were installed on the bottom of the hole. Above the hydraulic jacks a steel plate with an outer diameter of 1.75 m was placed. In order to better simulate the dry upper bentonite block in a deposition hole a bentonite block with correct dimensions was placed on top of the steel plate. The buffer block was pushed upwards by the hydraulic jacks during the test, simulating the swelling bentonite from a deposition hole. A detailed drawing showing all main components is provided in Figure 2-2.

The test was performed in the TASS (T = tunnel, AS = Äspö site, S = letter ID for the tunnel in question; this nomenclature is used in the SKB database, Sicada) tunnel at Äspö HRL at a depth of about 420 m below ground. The tunnel was backfilled with bentonite blocks and pellets. The blocks were produced at Höganäs Bjuf with bentonite from the Asha-2012 delivery, which is an Indian bentonite. The blocks were produced with an average dry density of 1,642 ± 11 kg/m^3. The pellet filling was made of 6 mm extruded pellets also from Asha bentonite. See Arvidsson et al. (2015) and Andersson and Sanden (2012) for detailed descriptions. The installation of the backfill blocks had a length of 12 meters and the artificial deposition hole was placed in the centre of the block masonry i.e. 6 meters from the tunnel end.

A number of measurements were done before, during and after the test.

- The force on the steel plate was applied and measured by 4 hydraulic jacks.
- The displacement of the steel plate was measured by 4 displacement transducers placed under the steel plate.
- The maximum vertical pressure was measured in 41 points on the blocks (see Figure 2-3).
- The positions of 28 blocks were measured before and after the test (see Figure 2-3).
- The total stress on the rock surface was measured in 5 points in the roof and the rock wall (see Figure 2-3).
- The rock contour and the distance between the rock surface and the blocks were measured.

The rock contour was rather uneven since the drift was excavated by drill and blast. Figure 2-4 shows the measured rock contour in relation to the blocks in section 4.

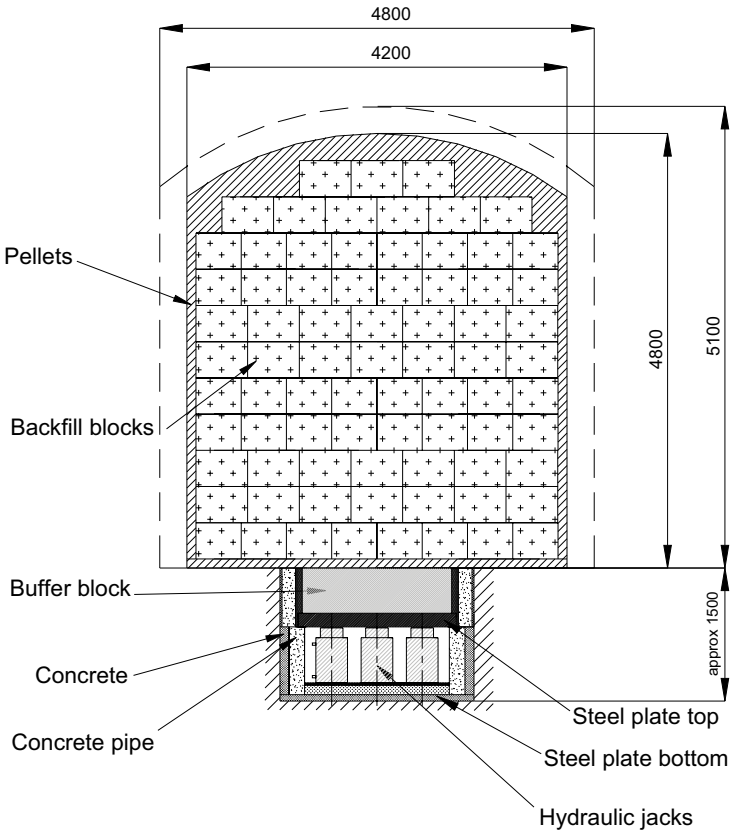

Figure 2-1. *Schematic drawing showing the principle test design.*

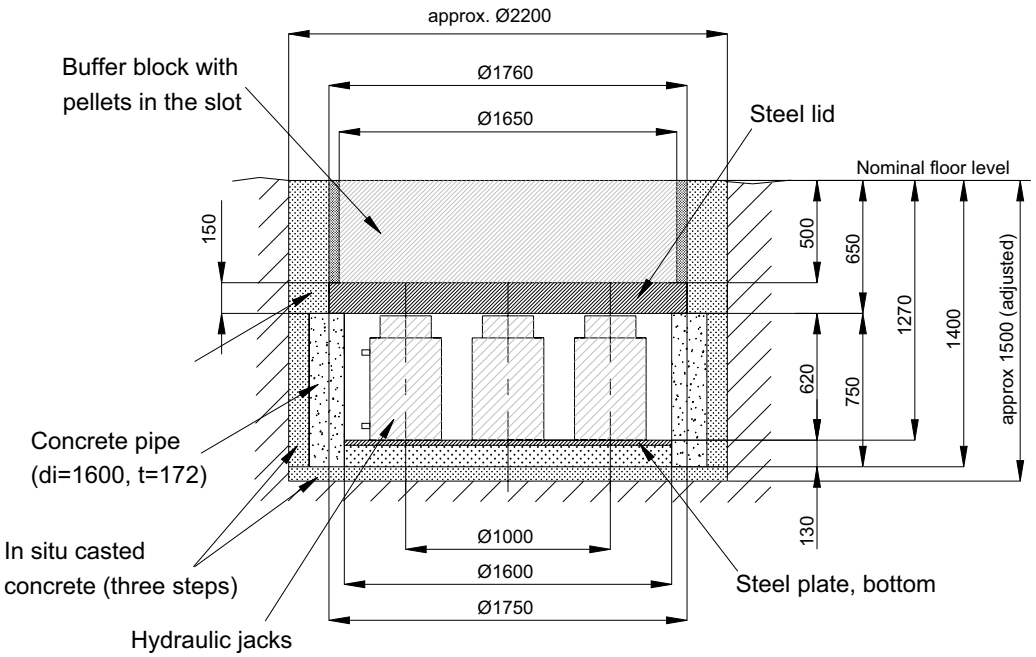

Figure 2-2. *Detailed description showing the main components of the test design.*

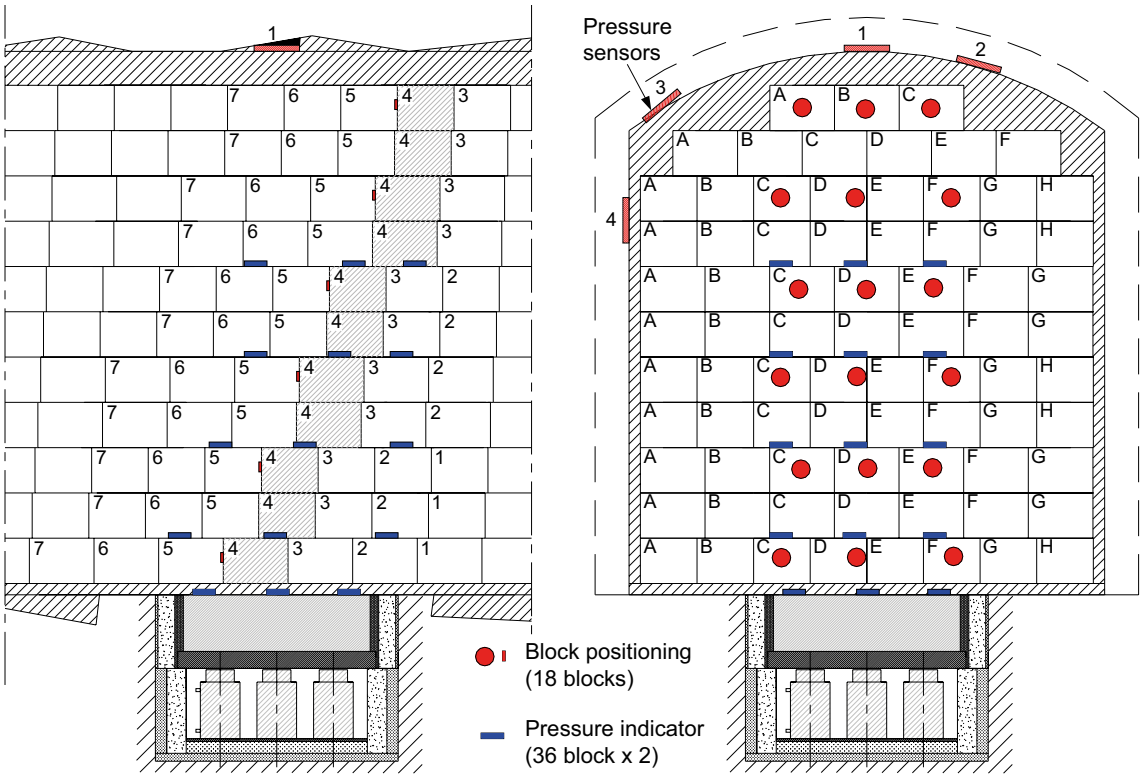

Figure 2-3. *Schematic drawing showing the block layers above the simulated deposition hole. The pressure indicators (blue) were placed at the top of the buffer block and between the blocks in the block masonry. The positions of eighteen blocks (red dots) in the inclined layer 4 (hatched) were determined using a total station. The location of pressure sensors 1–4 are shown in the figure. Pressure sensor 5 is placed in the ceiling 2 m from the centre of the deposition hole.*

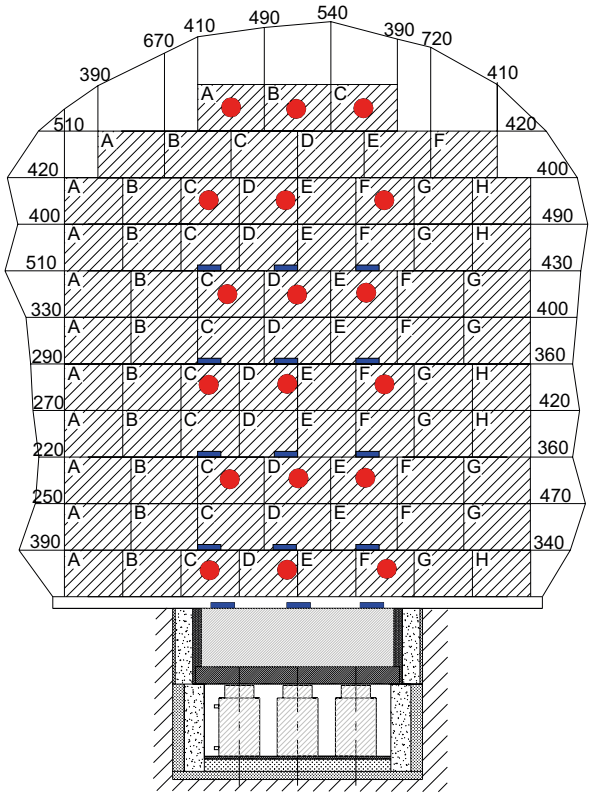

Figure 2-4. *Schematic drawing showing the measured distances between block and rock surface for block layer 4 above the deposition hole.*

2.2 Important results

The upwards displacement of the steel plate was made by applying the load in steps by moving the steel plate upwards either 5 or 10 mm and having a certain relaxation time (15 minutes) between each step. 15 minutes were chosen since most of the relaxation was completed after that time.

The results of the measured total average vertical stress on the steel plate and of the measured total stress on the rock surface are plotted in Figure 2-5 and Figure 2-6 as function of the displacement of the steel plate.

Figure 2-5 clearly shows a maximum of the vertical stress on the steel plate after about 80 mm displacement and a constant residual stress after about 10 cm displacement. This indicates that there has been failure in the block stack, which is confirmed during excavation of the blocks. Figure 2-7 shows a photo of the centre of the block stack just above the simulated deposition hole. A large number of blocks in the centre of the stack have cracked.

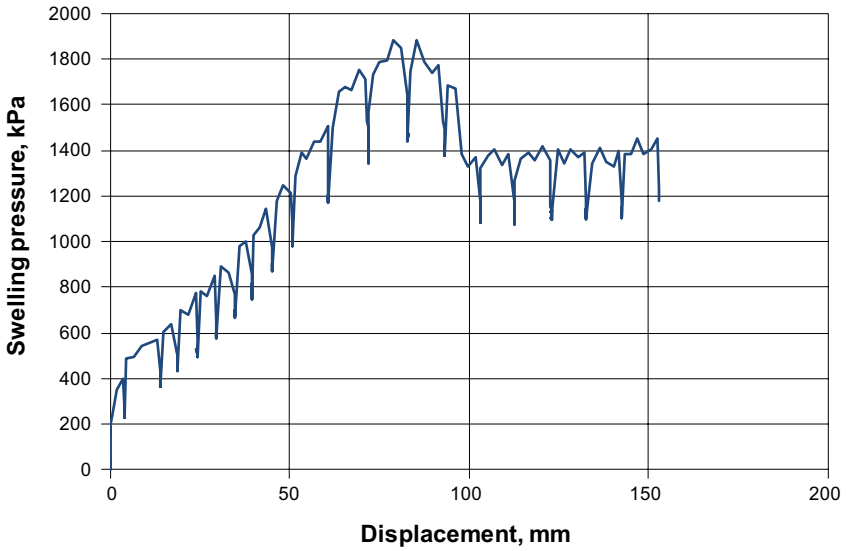

Figure 2-5. *Vertical total stress (simulated swelling pressure from the buffer) on the steel plate plotted as a function of the upwards displacement of the steel plate.*

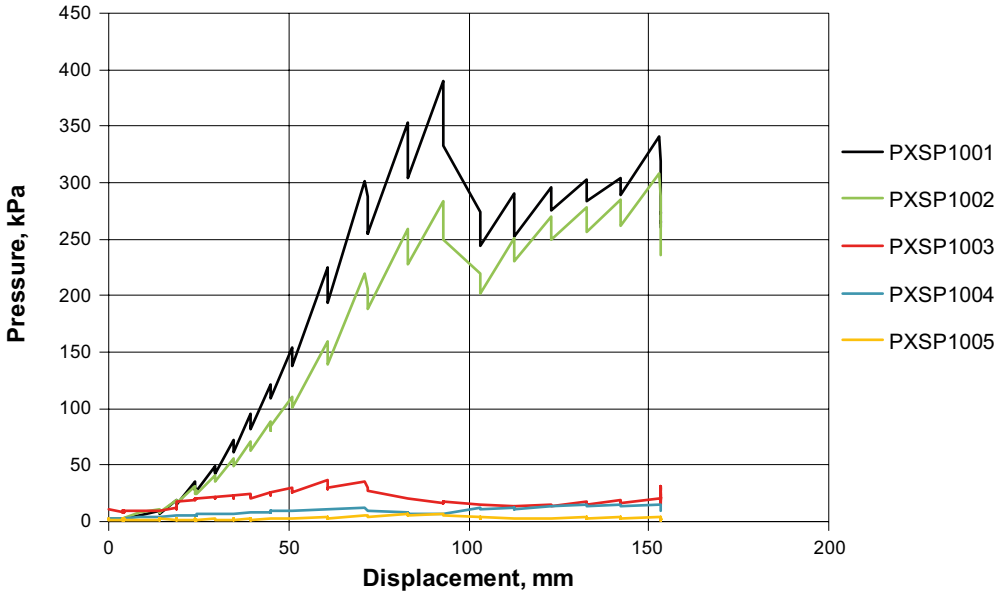

Figure 2-6. *Pressure registered at the sensors placed on the rock ceiling and walls plotted versus the upwards displacement of the steel plate.*

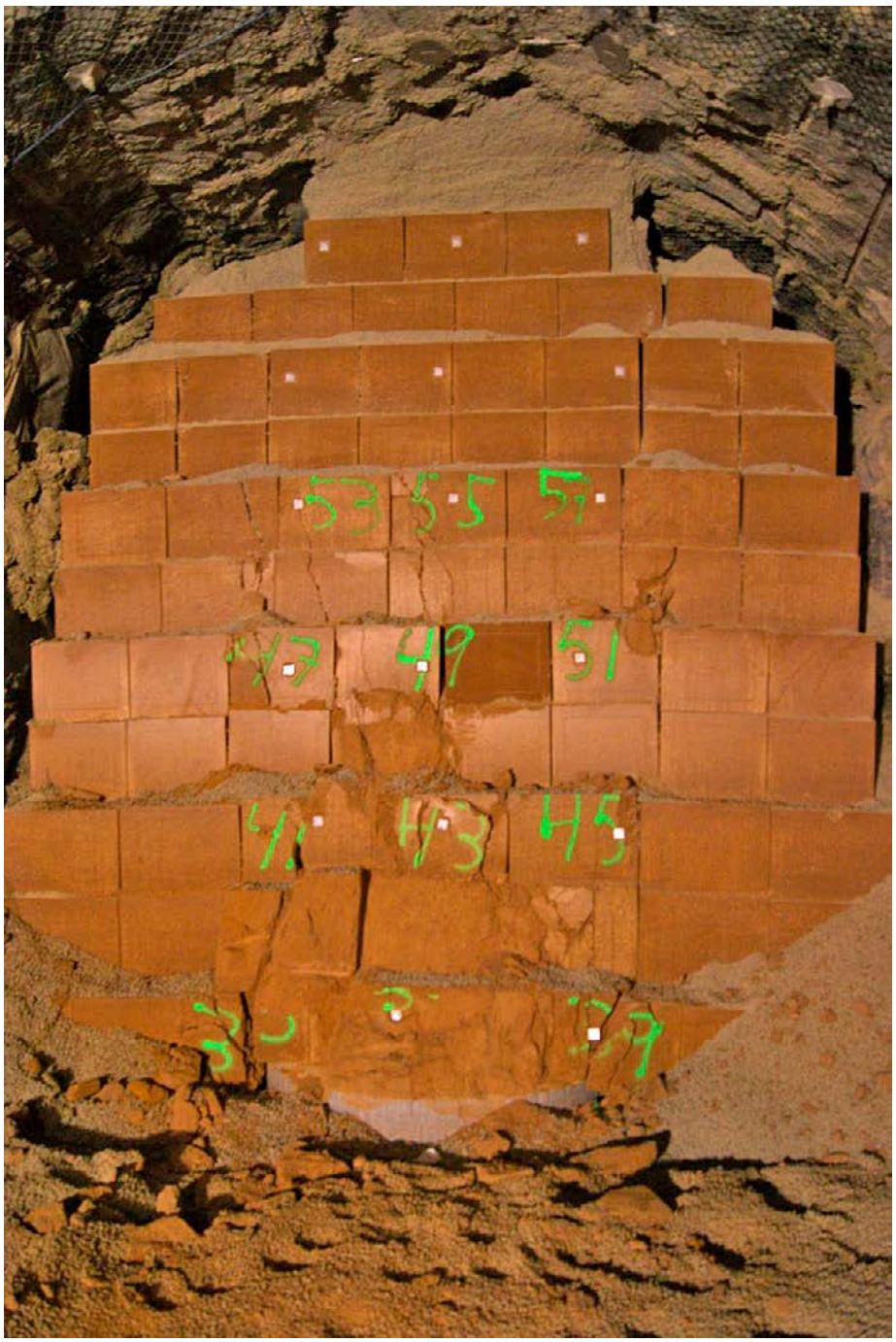

Figure 2-7. *Photo of the block stack above the simulated deposition hole taken during excavation showing the displacements of the blocks and cracking of some of them.*

3 Modelling of the buffer swelling test with Abaqus

3.1 Modelling

3.1.1 General

The finite element code Abaqus was used for earlier calculations performed by Börgesson and Hernelind (2014). Abaqus is a code that includes special materials models and it can be used for modelling rock and soil in geological formations. The theoretical background concerning the code used has been described in detail in Börgesson and Hernelind (2014) and is not repeated in this document.

The bentonite block masonry and the bentonite pellets in the test have been modelled in the same way as used for modelling the upwards swelling of the bentonite in a deposition hole towards a dry tunnel (Börgesson and Hernelind 2014). The same parameter values have been used for the reference case. In addition a sensitivity analysis has been done with a number of additional calculations, where the parameters of the pellet filling and the properties of the block masonry have been changed. This analysis is not included in the present report but will instead be part of another report (Börgesson and Hernelind 2017)

The results showed that failure with cracking of many blocks have occurred, but this process is not possible to model accurately with today's knowledge so only the results up to 8 cm displacements have been used for evaluation and comparison with measurements. The calculations were only run to 10 cm displacement.

3.1.2 Material models

There are three different parts included in the dry backfill, namely the blocks, the joints between the blocks and the pellet filling. In addition one buffer block with the same dimensions and properties as the buffer blocks in a deposition hole is included

Block section of masonry

The backfill blocks in the masonry will according to the reference design in the production line report be compacted with a water content of 17 % to a dry density of 1 700 kg/m^3. Measurements of the elastic properties of potential backfill materials (e.g. Asha and IBECO-RWC-BF (Johannesson 2008)) have yielded fairly equal results. The blocks are very stiff compared to the pellet filling and the joints so the results are not very sensitive to the elastic properties of the blocks.

The backfill blocks are modelled as a linear elastic material with the following properties:

E = 245 MPa

ν = 0.17

Initial average stress p_0 = 0 MPa

Although the blocks used in the test differed somewhat from the reference blocks (mainly by having a lower dry density) the properties of the reference blocks were used in the modelling presented here as the base case.

Buffer block

The buffer block that is displaced upwards is allotted the same properties as the backfill blocks.

Pellet section

The parts filled with pellets are modelled with linear elasticity and Drucker-Prager plasticity. The plastic behaviour is modelled with Drucker-Prager plasticity. For detailed descriptions see Åkesson et al. (2010) and Börgesson et al. (1995).

Drucker-Prager plasticity:

$\beta = 55°$ (corresponds to a Mohr-Coulomb friction angle of $\phi = 30°$)

$d = 52$ kPa

$\psi = 0°$

Yield function

q **(kPa)**	εpl
100	0

Von Mises' stress q is here defined as

$$q = (((\sigma_1-\sigma_3)^2 + (\sigma_1-\sigma_2)^2 + (\sigma_2-\sigma_3)^2)/2)^{1/2} \quad (3\text{-}1)$$

Elastic properties:
$E = 3.9$ MPa (base case)
$v = 0.3$
Initial average stress $p_0 = 0$ MPa

The base case corresponds to the stiffness of a pellet filling that has not been compacted.

The compressibility of different pellets fillings have been tested and reported by Johannesson (2008) and Andersson and Sandén (2012). The E-modules used are evaluated from those measurements for an increase in stress from 0 to 2 MPa.

Joints between blocks

Since the bottom bed on which the blocks rest cannot be made as a completely plane or horizontal surface the backfill blocks will be placed slightly uneven in relation to each other. This means that there will be joints that are not even due to slightly inclined blocks that also have slightly different heights. The properties of these joints between the blocks are not known but they will have compression and friction properties that deviate significantly from the properties of the blocks.

The following properties have been applied to the joints (both horizontal and vertical):

- Average joint thickness: 4 mm (fictive)
- Compression properties: The normal pressure is defined by an exponential relation by defining the pressure (zero) at zero compression (initial position) and the pressure 10 MPa when the joints are closed. Due to the exponential relation urther compression will quickly increase the compression stress and thus prevent large overclosures. However, the actual pressure will never be near such a high value.
- Friction angle $\phi = 20º$

Figure 3-1 shows the stress-compression relation that has been used for the joints.

Rock

The rock is modelled as an elastic material with high stiffness.

$E = 1.85 \times 10^8$ kPa
$v = 0.3$

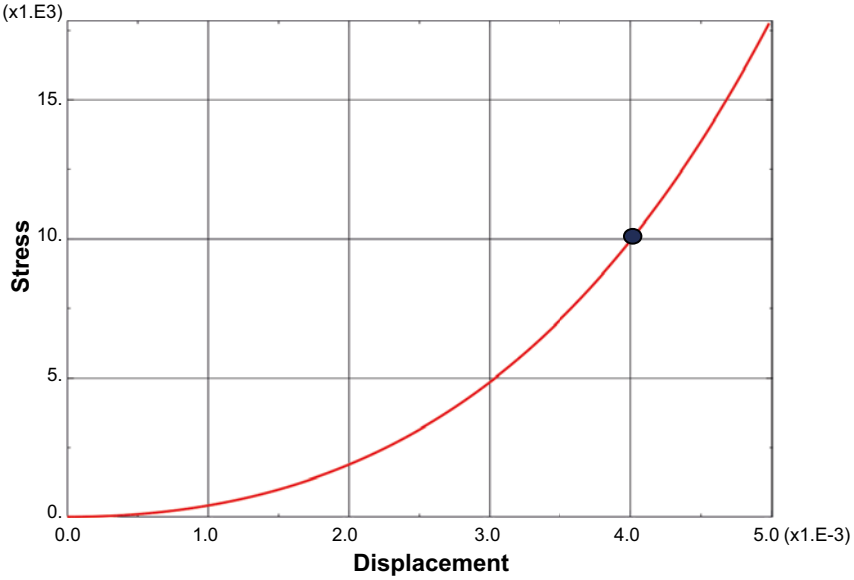

Figure 3-1. *Mechanical model of the joints between blocks. The displacement or compression (m) of the joint is plotted as a function of the total stress (kPa) perpendicular to the joint. After 4 mm compression the 4 mm joint is closed.*

3.1.3 Element mesh

The backfill block masonry is placed with the pattern that is referred to as the reference backfill design and used in earlier calculations. This means that the same geometry could be used for the calculations as was used by Börgesson and Hernelind (2014). The exact position of the simulated deposition hole was not defined with any precision so it was decided to assume that it was placed in the centre at the same location as used in those earlier calculations.

The model contains approximately 14 000 elements and 35 000 nodes. Both 8- and 20-node bricks were used.

Figure 3-2 shows the geometry and the mesh of the block masonry.

The thickness of the pellet filling has been set as follows:

- At the crown of the roof: 460 mm
- At the walls: 100 mm
- At the floor: 80 mm

There were some problems with running the calculations and receiving convergence. The problems were localised to the 90° edge contact between the buffer block and the pellet filling in the floor were large strains took place. In order to reduce the convergence problems contact surfaces were applied in the pellet filling in the floor as a continuation of the modelled deposition hole. By doing so the pellet filling could deform without large strains in the contact zone.

3.1.4 Boundary conditions

The following boundary conditions are applied:

- The vertical boundary planes are symmetry planes and free to move parallel with the plane and fixed perpendicular to the plane.
- The horizontal boundaries are fixed.

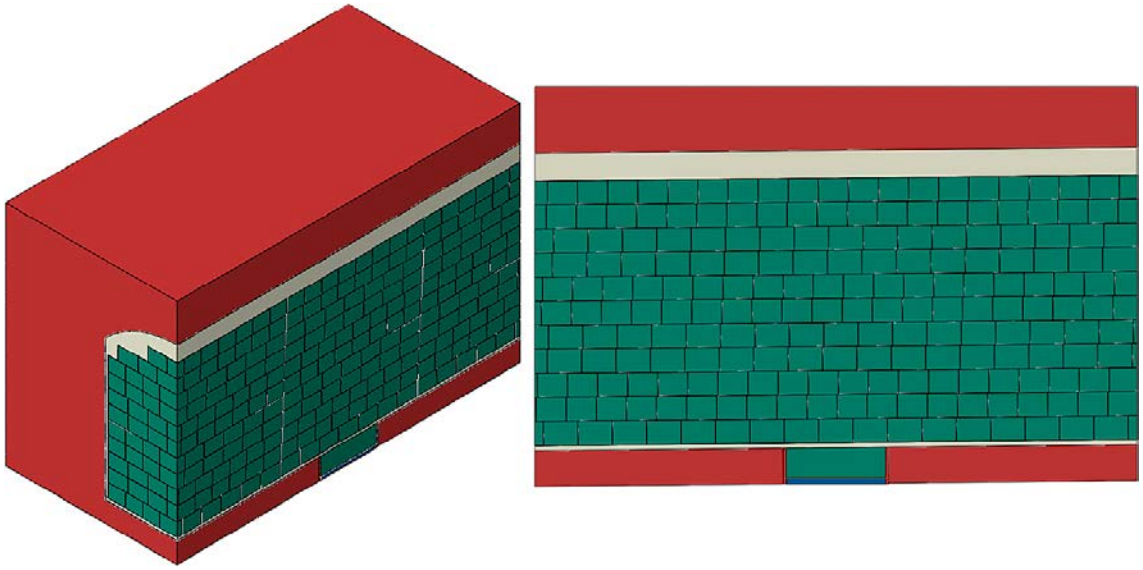

Figure 3-2. *Geometry for the calculation. Each block is one element. The mesh of the other materials is not shown.*

3.1.5 Contact surfaces

The interaction between the pellets filling and the rock has been defined by contact surface allowing opening/closing in the normal direction and with friction in the tangential directions. The friction has been modelled with Mohr Coulomb's parameter friction angle ϕ and without cohesion c.

$\phi = 30\ 01°$

$c = 0$

This friction angle corresponds to the friction angle of the pellets filling $\beta = 55°$ in the Drucker-Prager model, which means that the contact surfaces are considered rough. See Appendix F in Glamheden et al. (2010).

The contact surfaces are made not to withstand tensile stress, which means that the contact may be lost and a gap formed between the surfaces.

Another property of the contact surface is the so called "slip tolerance", which describes the required slip to reach full friction. This parameter has been set to 1 mm. Below 1 mm slip the friction stress is proportional to the slip and normal pressure. For slip more than 1 mm the friction stress is proportional only to the normal stress with the coefficient of friction equal to 1.42.

3.1.6 Calculations

The calculations are purely mechanical. The steel plate has been displaced vertically until the total displacement 100 mm. The calculations included a technique for facilitating the convergence conditions by introducing damping forces.

Gravity has not been included in the calculations so an extra pressure corresponding to the own weight of the block masonry should be added in the final evaluation. With the total height of 4.4 m and the density of the blocks $\rho = 1\,989$ kg/m^3 the additional pressure is $\Delta\sigma = 87.5$ kPa.

In the sensitivity analysis the influnece of varying the stiffness (or thickness) of the pellet fillings in the floor, ceiling and walls and the stiffness of the joints has been analysed. These results are not shown here but in Börgeson and Hernelind (2017).

3.2 Results for the reference case

3.2.1 Results after 10 cm displacement

At first the modelled stress and displacements etc. after 10 cm displacement of the steel plate will be described. Then the stress-deformation plots will be shown and compared with the measurements. Finally an analysis of the cracking of the blocks and the consequence of not including it in the modelling will be made.

Displacements

Figure 3-3 shows the displacements in the block masonry after 100 mm total displacement of the steel plate. The figure shows that the pellet filling in the floor is compressed about 30 mm and the pellet filling in the roof 30–40 mm. The remaining compression (30–40 mm) takes place in the block masonry (in the joints).

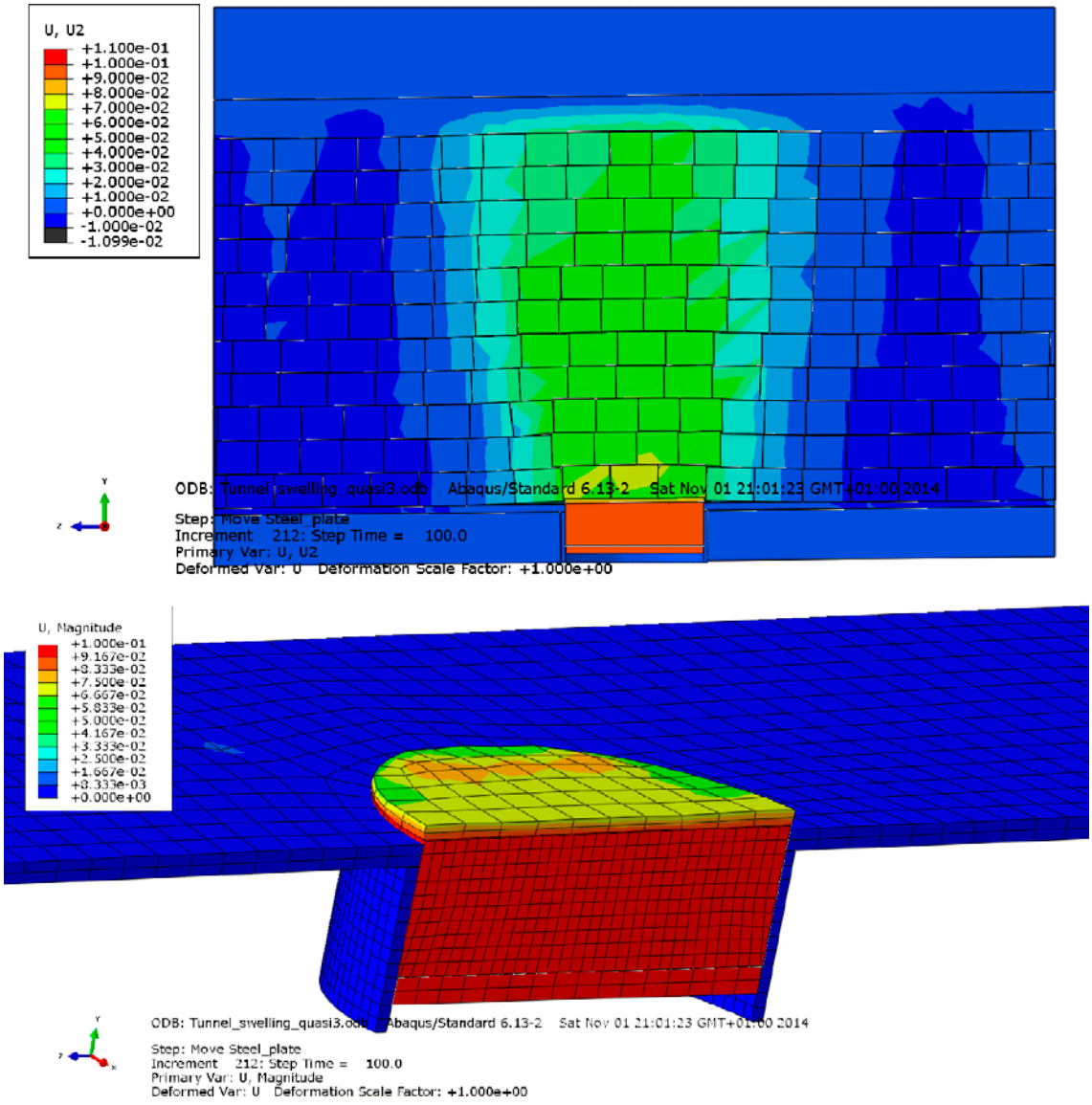

Figure 3-3. *Displacements (m) of the blocks in the masonry (upper) and a detail of the buffer block and the pellet filling above the buffer block. The upper figure presents vertical displacements and the lower total displacements*

Mises' stress

The Mises' stresses after 10 cm displacement are shown in 5 different sections located as illustrated in Figure 3-4.

Figure 3-5 to Figure 3-9 show the results.

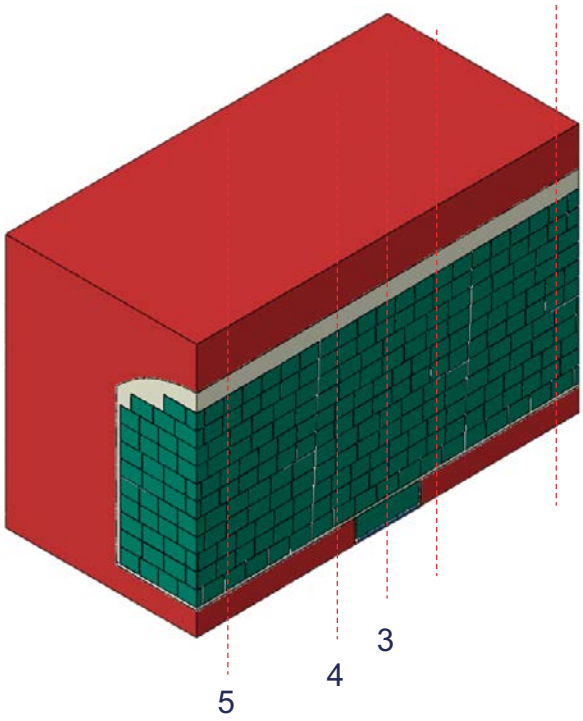

Figure 3-4. *Location of sections where the Mises' stresses are shown (Figures 5-3 to 5-7).*

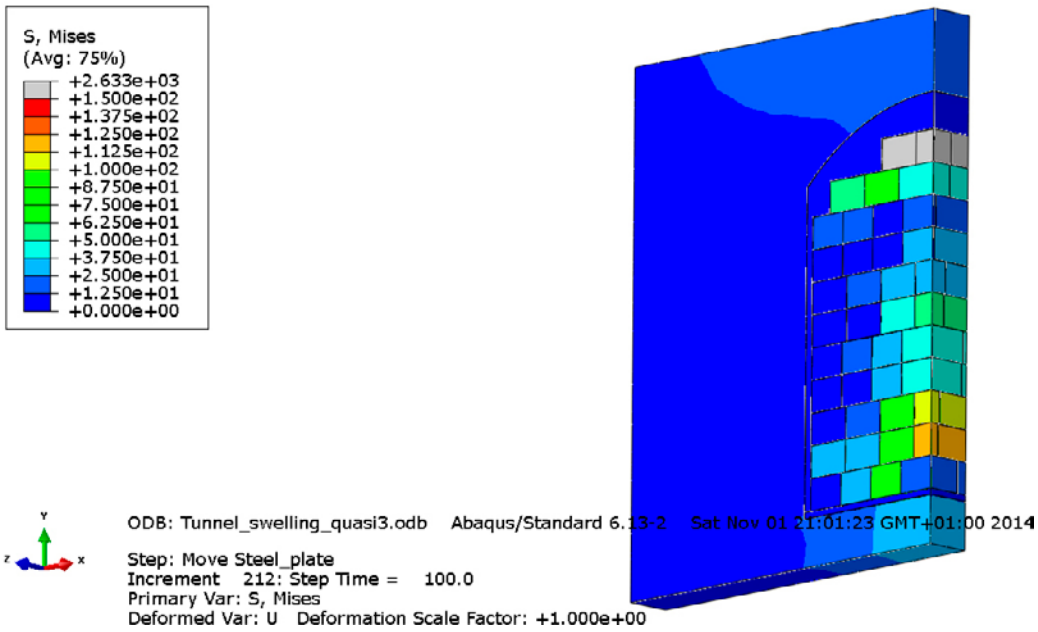

Figure 3-5. *Mises' stress (kPa) in section 1.*

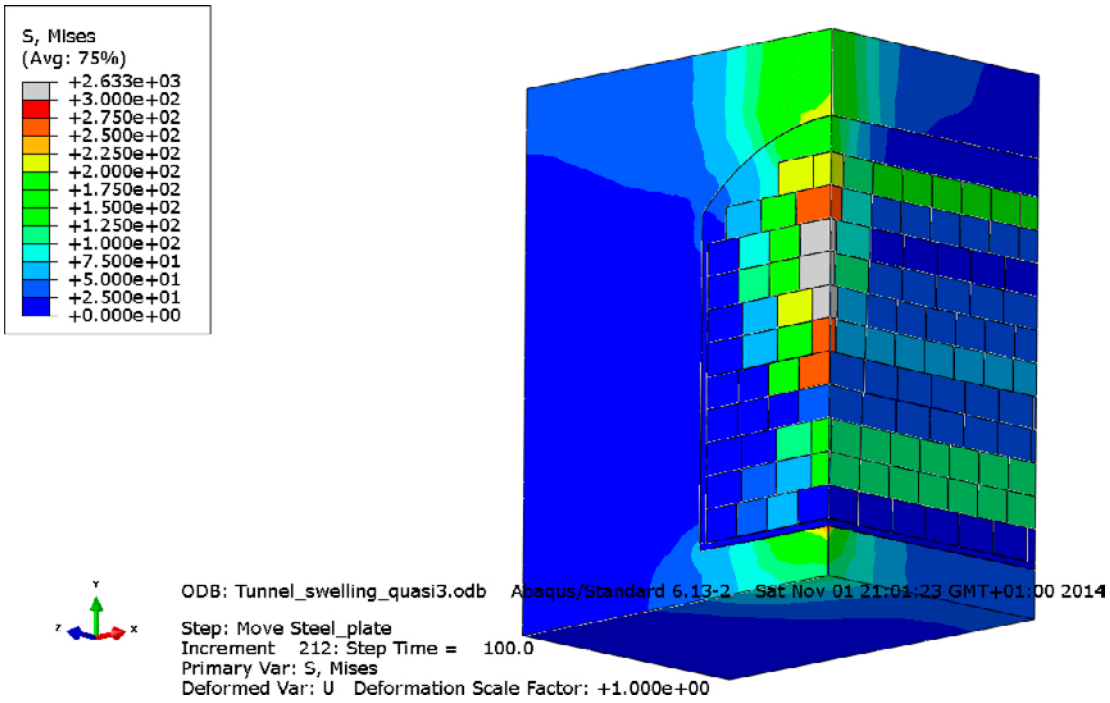

Figure 3-6. *Mises' stress (kPa) in section 2.*

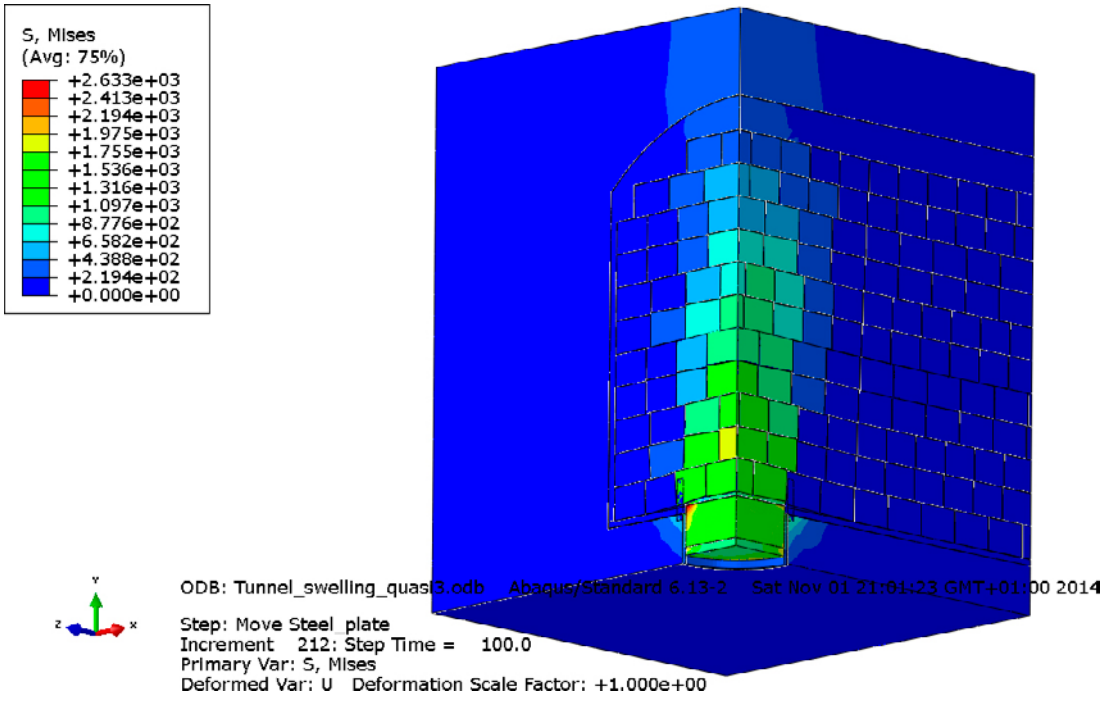

Figure 3-7. *Mises' stress (kPa) in section 3.*

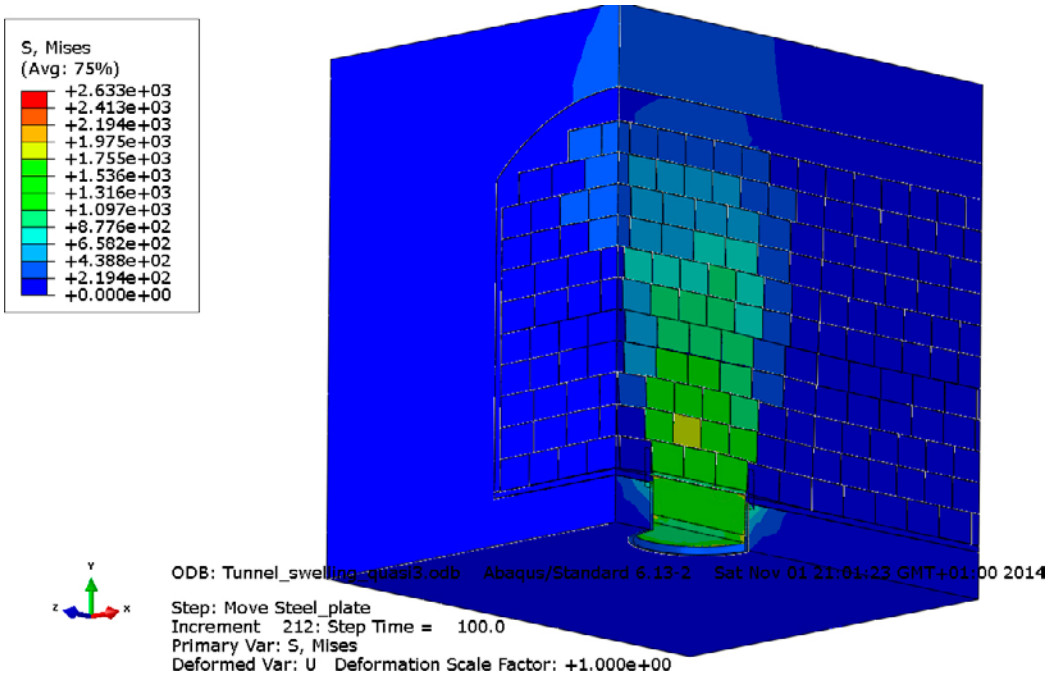

Figure 3-8. *Mises' stress (kPa) in section 4.*

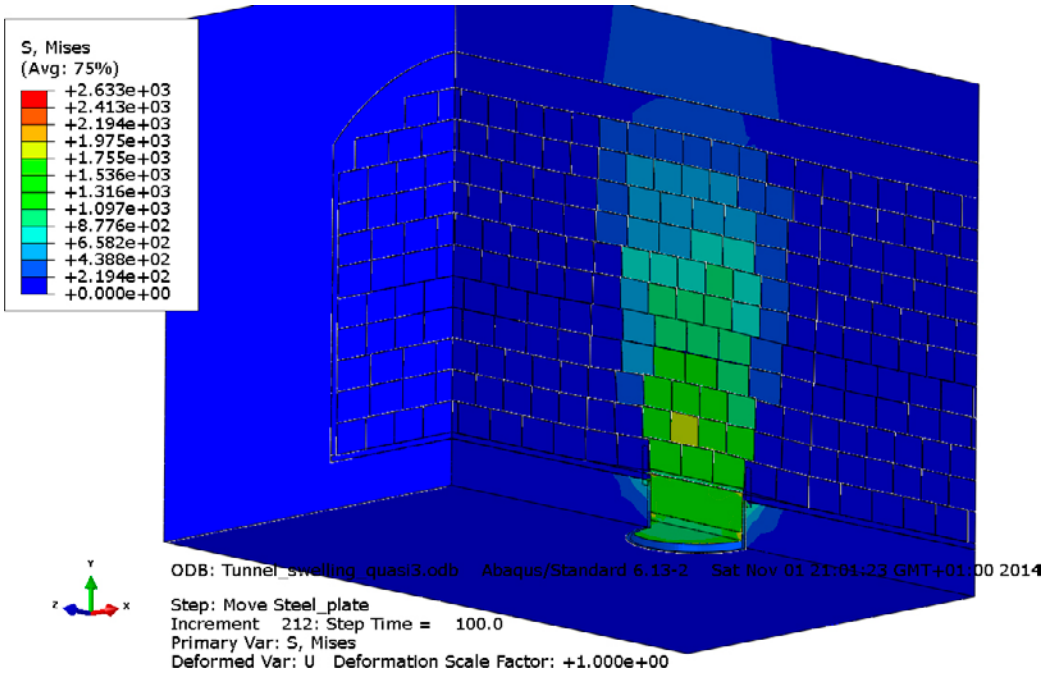

Figure 3-9. *Mises' stress (kPa) in section 5.*

The figures of the Mises'stresses show a number of interesting results.

- Very high stress 2.6 MPa are found in the upper corner of the buffer block.
- The highest stress in the backfill blocks seems to be about 1.8 MPa.
- The high stresses seem to be concentrated to a column just above the simulated deposition hole.
- Outside this column the stress is lower than about 300 kPa.
- There is some lateral stress spreading that results in a stress decrease with distance from the buffer block.
- There are no blocks with Mises' stress higher than 900 kPa in the upper three levels of backfill blocks.

It should though be noted that the stress in the backfill blocks are average stress since the blocks constitute of one element each. Local stresses in the blocks may be higher.

Vertical stresses

Some results of vertical stresses are illustrated in Figure 3-10 and Figure 3-11. Figure 3-10 shows the stresses lower than 1 MPa in the vertical symmetry plane along the tunnel axis. The blocks with higher stress are separated and shown in Figure 3-11. Compression stresses are negative.

The vertical stresses are very similar to the Mises' stresses since the lateral stresses are rather small.

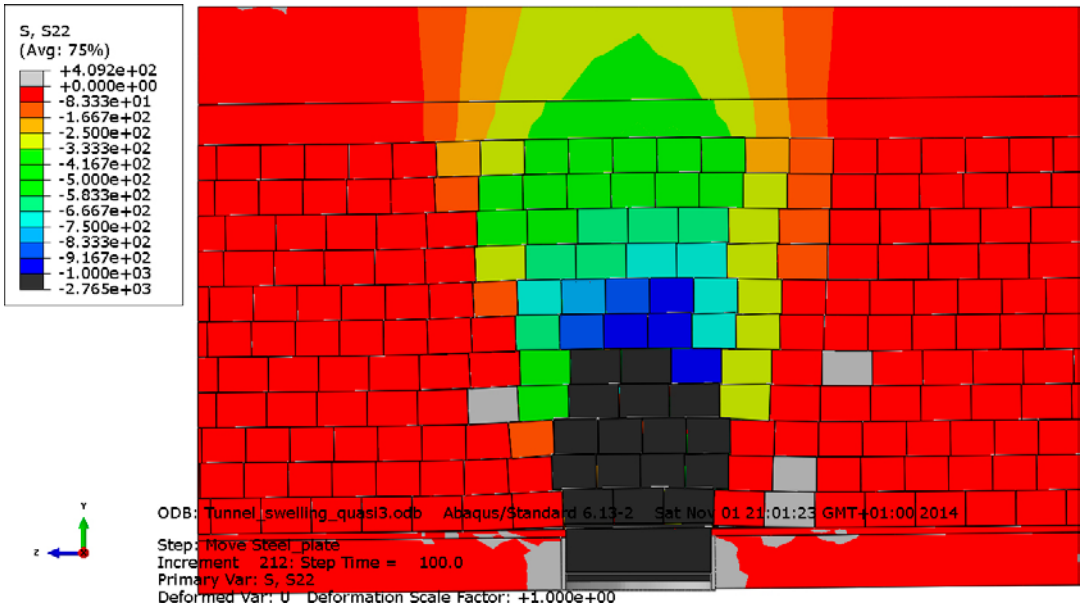

Figure 3-10. *Vertical stress (kPa) after 10 cm displacement. Blocks with higher stress than 1 MPa are painted black.*

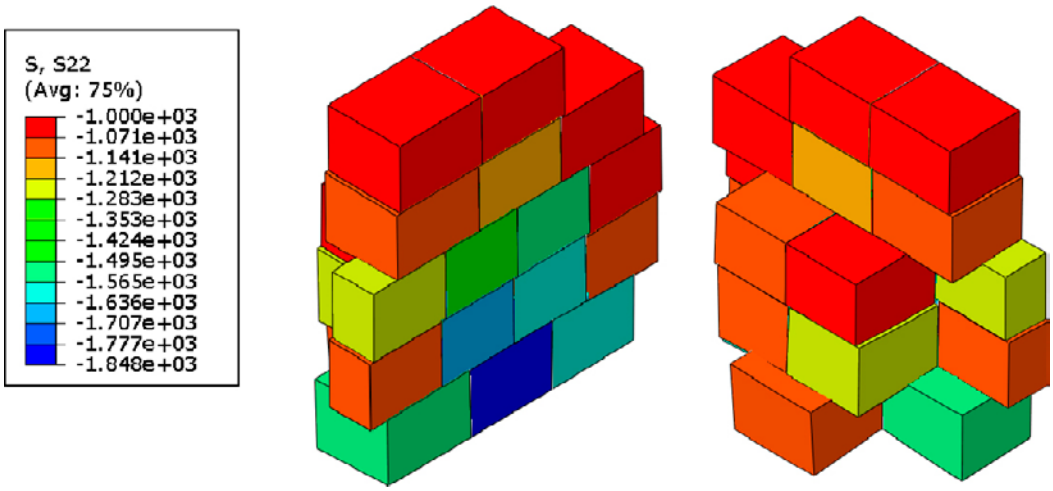

Figure 3-11. *Vertical stress (kPa) in the backfill blocks that have stresses higher than 1 MPa.*

Stresses on the rock surface

The normal stresses against the rock surface are shown in Figure 3-12 and Figure 3-13.

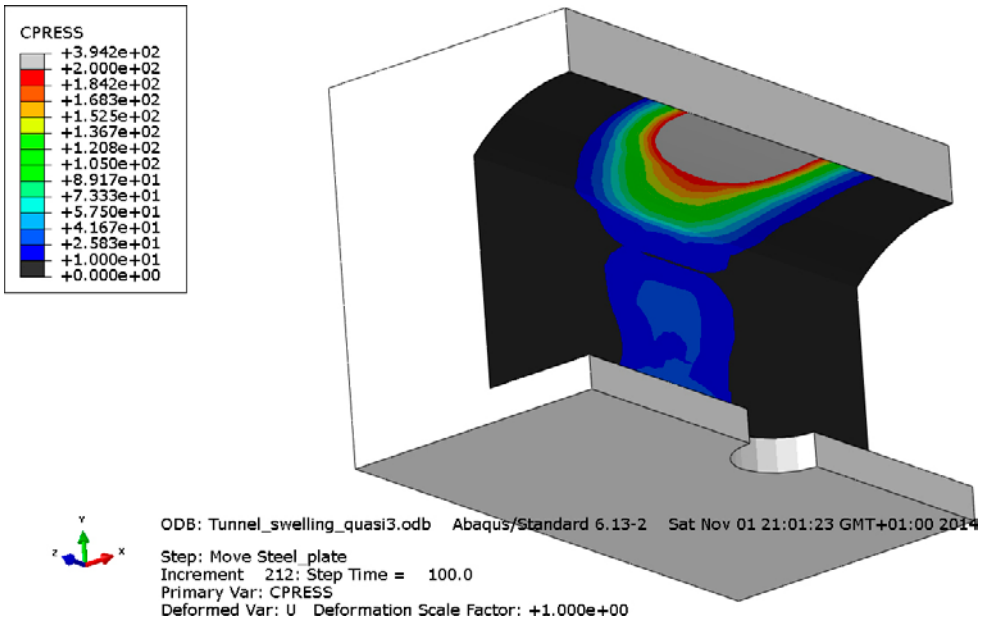

Figure 3-12. *Normal stress (kPa) against the rock surface for stress magnitudes between 10 kPa and 200 kPa.*

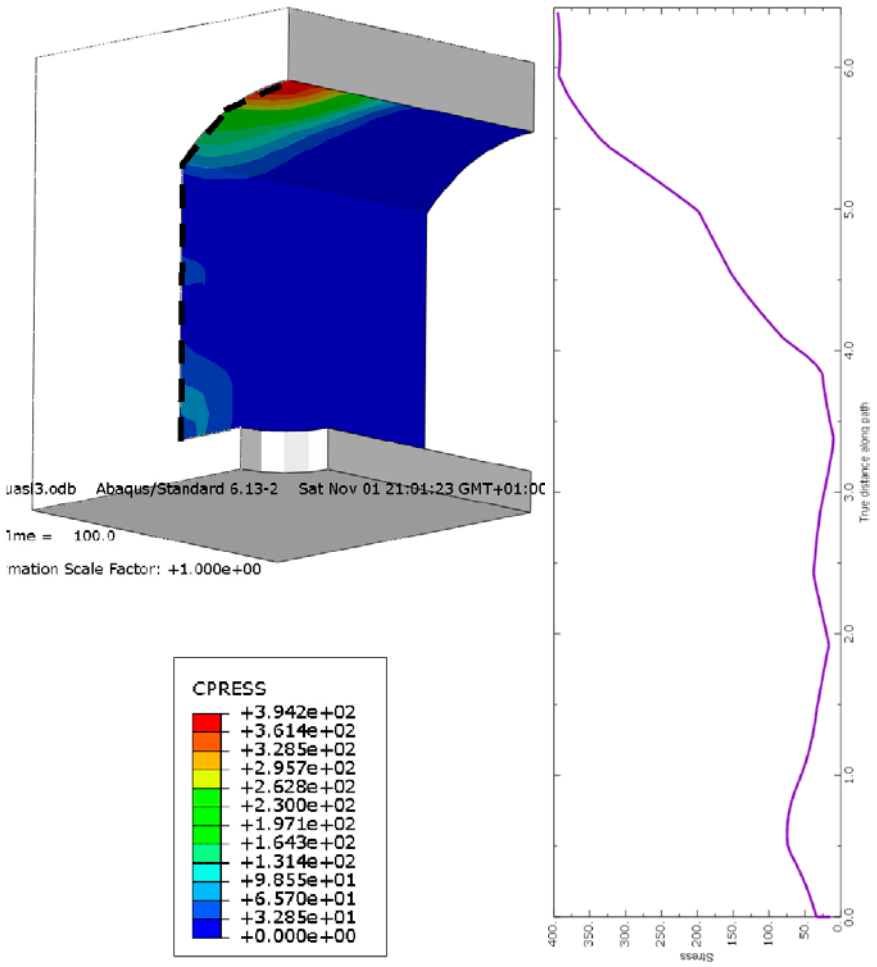

Figure 3-13. *Normal stress (kPa) against the rock surface (contact pressure). The right figure shows the stress distribution along the hatched line shown in the left figure. Normal stress (KPa) (x-axis) vs. distance (m) along the rock wall (y-axis).*

The results show that the stresses against the rock surface are quite small. The largest stress is naturally in the crown of the ceiling just above the centre of the simulated deposition hole, where the maximum stress is almost 400 kPa. The stresses on the walls are generally lower than 50 kPa except locally close to the floor.

3.2.2 Stress evolution

The modelled evolution of stresses on the steel plate and in the measuring points on the rock surface is shown in Figure 3-14.

3.2.3 Comparison to modelled measure results

The modelled evolution of stresses on the steel plate and in the roof is compared with the measured in Figure 3-15 and Figure 3-16.

The modelled total stress evolution on the steel plate shows remarkable good agreement with the measured stress up to about 80 mm displacement. The measurements show stress relaxation that originates from the loading sequence that was done stepwise with 15 minutes rest between the load steps.

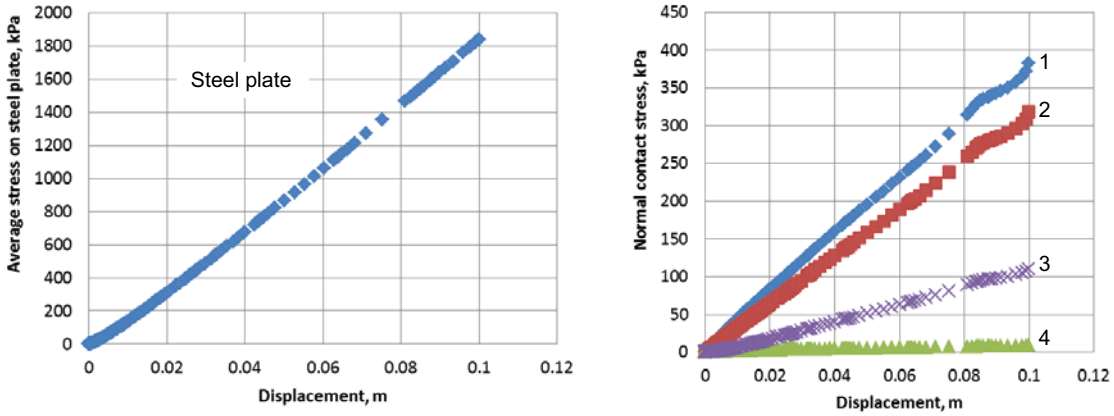

Figure 3-14. *Modelled normal stress distribution as function of the displacement of the steel plate. The average normal stress on the steel plate is shown in the left figure and the stresses on the rock surface in the right figure. See Figure 3-2 for the location of the stress gauges.*

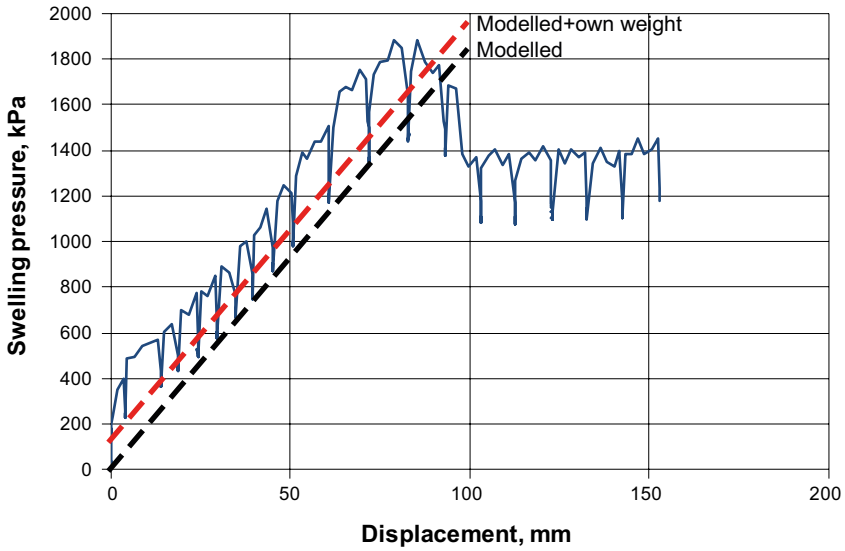

Figure 3-15. *Modelled and measured evolution of total vertical average stress on the steel plate. The own weight of the backfill block is also added in the figure.*

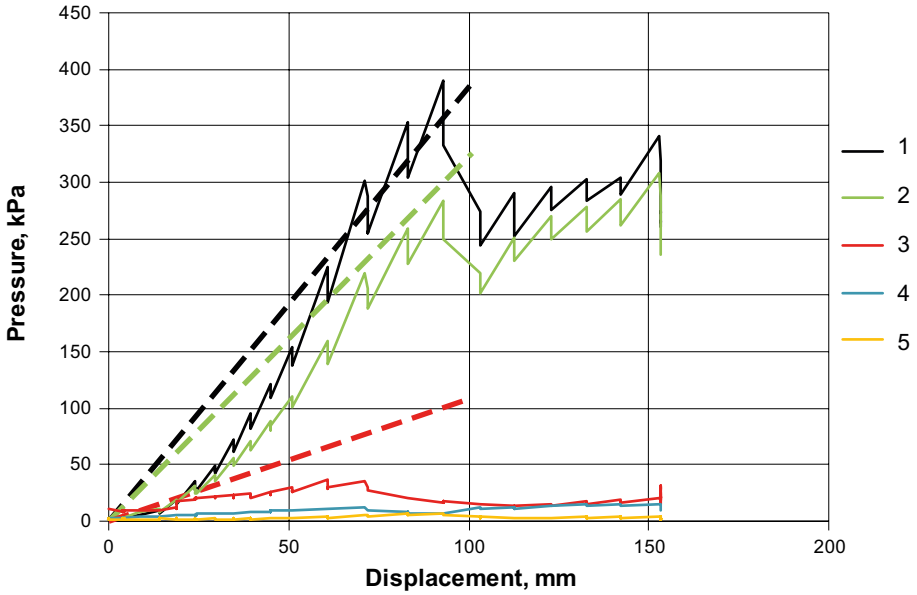

Figure 3-16. *Modelled and measured evolution of total stress perpendicular to the rock surface in the central cross section. The location of the pressure sensors are shown in Figure 2-3. Sensor 5 is located in the crown 2 m away from the central section.*

After 80 mm there the measurements show as mentioned before a peak value and a decrease until a constant residual stress is reached. The reason for this is judged to be failure of some of the backfill blocks, which is confirmed by other measurements and observations after the test. This failure is not modelled since it is not included in the material model so what happened after 80 mm displacement cannot be used for evaluation of the modelling.

The modelled and measured stresses in the ceiling (transducers 1 and 2) and in the wall (4) also agree very well while the modelled stress at the corner between the wall and the roof (3) is higher than measured.

It is also interesting to compare the modelled and measured compression of the three different parts. Figure 3-3 showed that about 30 % of the compression took place in the pellet filling in the floor and about 35 % of the compression took place in both the pellet filling in the ceiling and in the block masonry (mainly the joints). According to the measurements (Sandén et al. 2017) more than 50 % of the compression took place in the block masonry and the rest in the two pellet layers but those measurements were done at excavation after 15 cm displacement i.e. they included 7 cm compression after block failure so the comparison halts.

3.2.4 Block cracking

At excavation it was seen that many blocks above the simulated deposition hole were cracked. Figure 3-17 shows modelled vertical stress in the blocks after 100 mm displacement and a photo of the block masonry in the centre section taken during excavation.

The measured compression strength of the blocks is according to Sandén et al. (2017) between 1 200 and 2 000 kPa with an average of about 1 600 kPa. Looking at the location of the blocks that have been fractured and the modelled vertical stress all block with the vertical stress higher than about 750 kPa are cracked. Considering that the test was run to 15 cm displacement but the simulation only to 10 cm a simple estimate might be that all blocks with vertical stress higher than about 1 125 kPa would be cracked. However, cracking of some blocks may increase the load of blocks located over the cracked blocks so the comparison is halting.

More interesting proof is the good agreement between the in average measured compression strength σ_c = 1 600 kPa and the maximum vertical stress from the steel plate which also was about 1 600 kPa.

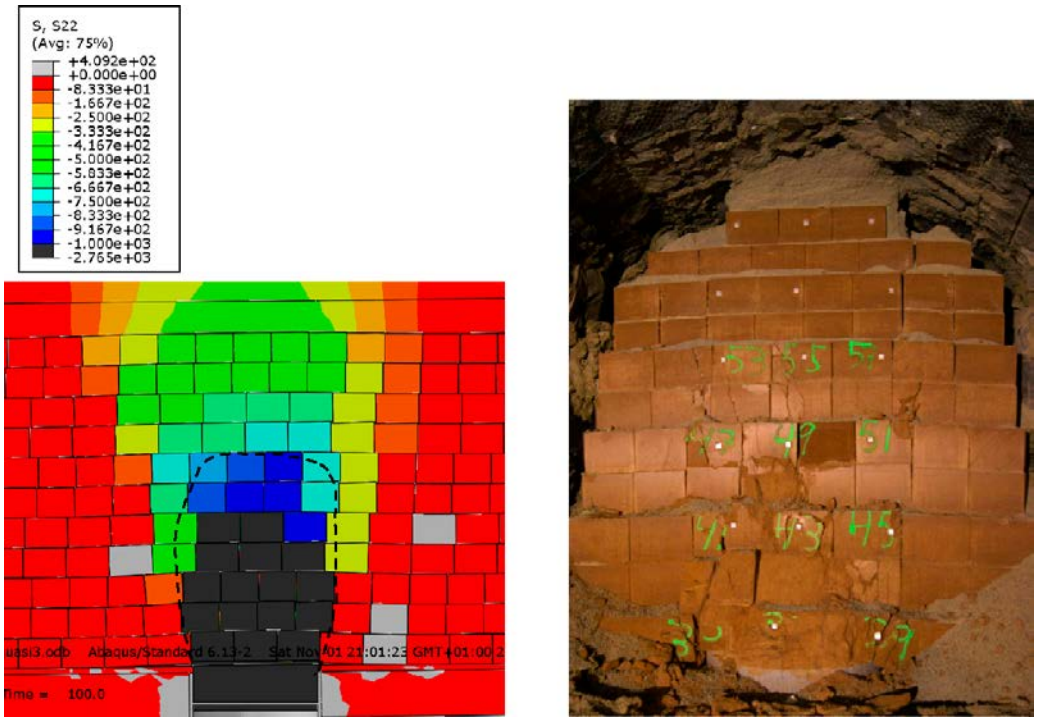

Figure 3-17. *Modelled vertical stress in the backfill blocks after 10 cm displacement and picture taken at the central part after excavation of half the test.* σ_c *= compression strength and* σ_t *= tension strength of the blocks measured in laboratory.*

3.2.5 Conclusions

The swelling test was modelled with the same technique and the same material models and properties as used for the earlier calculations of the effect of upwards swelling. The results showed surprising agreement with measurements up to 80 mm displacement where the backfill blocks in the test started cracking. The blocks that had cracked were also the blocks with the largest stresses. In addition the vertical stress from the steel plate had the same maximum stress as the measured average compression strength of the backfill blocks.

In addition, sensitivity analysis on the effect of different parameters (pellet stiffness and thickness and gap widths/stiffness) were performed, the results of which are presented in Börgesson and Hernelind (2017).

3.3 Discussion of the results with Abaqus

The Buffer swelling test, simulating upwards swelling of the bentonite buffer into a dry backfilled tunnel, has been modelled with the FE-code Abaqus. The same material models and parameter values and the same modelling technique have been used as for the previous done calculations of buffer swelling effects for design purpose (Börgesson and Hernelind 2014). No adaption of parameter values or material models, in order to have a result that agrees as much as possible with the measurements, has been done.

The results of the modelling agreed very well with the results of the measurements in the test up to the upwards displacement 80 mm. For the rest of the test up to the displacement 150 mm there was no increase in stress but instead a decrease and a residual constant stress for the last 50 mm displacement. It was concluded and verified at termination and excavation after the test that the reason for the behaviour after 80 mm displacement was cracking of the backfill blocks. Since cracking could be included in the modelling because relevant models have not been developed and tested only the results up to 8 cm displacement can be used for evaluation of the modelling.

In spite of the good agreement between modelled and measured results a sensitivity analysis was done where the stiffness of the pellet filled slots (which could be translated to thickness of the slots) and the stiffness of the joints between the backfill blocks were varied but not reported here.

Analyses of the modelling and the test results in combination with results from laboratory tests made on the backfill materials have yielded a number of conclusions:

- The maximum pressure from the steel plate that was used to simulate upwards swelling of the buffer was about 1 600 kPa, which agreed well with the compressive strength of the backfill blocks. It was thus concluded that the cracking and failure of these blocks was the reason for the behaviour at larger displacements.
- The backfill blocks had lower density and water content than intended and the strength of these blocks was much lower than expected (Sandén et al. 2017). Since blocks with much higher strength (about 5 MPa) are easy to produce (Sandén et al. 2014) the conclusion is that the backfill blocks can be designed so that large failure caused by upwards swelling will not occur.
- According to the calculation the stresses in the blocks in the central part of the block masonry after 100 mm displacement exceed about 1 MPa in blocks that were cracked at termination of the test after 150 mm displacement. After 100 mm displacement the calculation showed that a few blocks had a vertical average stress exceeding 1.6 MPa. These results agree with the conclusion that the cracking of blocks and failure of the masonry started after about 8 cm displacement.
- The good agreement between modelled and measured results for the reference case up to 80 mm displacements showed that the material models and calculation technique used in previous calculations are well suited for this type of modelling.

4 Modelling of the buffer swelling test with PLAXIS finite element code

4.1 General

The software used for the calculations presented in this section has been the commercial software PLAXIS 3D rel. 2013. The package, specifically developed for geotechnical engineering problems, includes a wide range of constitutive models suitable for rock and soils.

Clay pellets have been modelled as a contiunuum, simulating its mechanical behaviour with a double hardening model. Interface elements have been selected for representing the interaction between the different parts of the model (blocks, pellets, buffer block, host rock). The uplift has been simulated by prescribed diplacement. See Section 4.2 for full details on the modelling.

A suitable constitutive model based on Hoek-Brown failure criterion has been selected for backfill blocks, assuming the original material for the backfill blocks as intact undisturbed rock with the mechanical properties assessed through laboratory tests.

The blocks have been explicitly modelled in a central region of the tunnel, whereas the blocks at the sides have been replaced by an equivalent continuum. The upward swelling from the buffer blocks has been modelled through a prescribed displacement applied on a disc of plate element.

4.2 Used constitutive models for volume, structural and interface elements with material parameters

The host rock is herein considered as a boundary condition, therefore it has been assumed as linear elastic material with high stiffness, thus equivalent to a rigid body in comparison to the typical compressibility of pellets and backfill blocks. However, in the light of the excavation technique (drill and blast) and the consequently non-planar geometry of the tunnel walls, the geometry has been modelled as envelope of the detailed survey through laser scan. Full detail of the assumed geometry is given in Section 4.3.

The metal plate on which the upward pressure was transferred to the upper part by hydraulic jack has been modelled implicitly through a prescribed displacement applied to a circular surface with the same diameter as the physical metal plate assuming that no (or very little) deformation occurred during loading.

On top of the loading surface a buffer block has been modelled, with linear elastic assumption as well, as it is experimental evidence that no failure occurred in the block during the whole loading process. The parameters of rock and buffer, assumed as linear elastic, are E' = 10 GPa and v' = 0.15. The unit weight does not play any role in this calculation therefore they were assumed weightless.

The pellet layer between the host rock and the backfill blocks has been modelled through the so-called Hardening Soil (Schanz et al. 1999), a double-hardening elastoplastic model which accounts for volumetric and deviatoric hardening. The set of model parameters used in the analysis is listed in Table 4-1, and they basically include physical properties, such as unit weight at natural water content and saturated medium γ and γ_{sat}, stiffness parameter at the conventional reference pressure of 100 kPa: E_{oed}^{ref} E_{50}^{ref} E_{ur}^{ref} with their exponent m, Poisson ratio in unloading-reloading v_{ur}, and strength parameters: effective cohesion and friction angle c', ϕ' and dilatancy angle at failure ψ. *TCO* defines a further yield function that prevents, if set to zero, the occurrence of tensile states. In order to identify the region where the ultimate compressive strength of the blocks was reached during loading, the interfaces between the blocks have been modelled through a so-called *ubiquitous joint* model Jointed Rock, included in the standard library of PLAXIS software.

By using the Jointed Rock model, one virtually incorporates the planes of failure, defined by the joints, within the constitutive model itself. On doing so, in this simplified approach the vertical interfaces were not explicitly included in the model, assuming only horizontal strata for each block layer. The used material parameter set is given in Table 4-2. The physical and strength parameters are the same as in Hardening Soil, with the difference that effective cohesion and friction angle are here defined along three independent possible failure planes. The stiffness parameter set is only limited to Young's moduli and Poisson ratios for an orthotropic medium.

Hence, the number of finite elements needed for the calculation was considerably reduced, thus enabling the identification of the volume involved in the propagation of failure points. The region where no or very little failure points was found has been replaced by a continuous medium. Full detail of the modelling procedure is given in the next section.

In the final run, where the blocks in the central region were explicitly modelled, elastic-perfectly plastic interfaces have been used for the block-block contact, whereas the elastic-perfectly plastic model based on Hoek-Brown failure criterion has been selected for the intact block material. Material parameters are listed in Table 4-3. Besides the usual physical properties and stiffness parameters, one needs to identify the uniaxial compression strength σ_{ci} and parameters related to the rock mass quality and its geological nature (m_i, *GSI* and *D*). Considering the validation purpose of this modelling exercise, all the material parameters have been assumed as in Leoni (2013) with the exception of Hoek-Brown parameters whose calibration has been based on the experimental results of compression tests on the blocks (Börgesson and Hernelind 2017). The uniaxial compression strength was taken directly form the test, whereas the mi, GSI and D parameters were identified by assuming intact, good quality argillaceous rock (Table 4-3). Bentonite pellets compressibility has been calibrated on the experimental values on the so-called Cebogel dry clay pellets.

Elastic-perfectly plastic interfaces have been assumed elsewhere at the interface between different materials. The block-block interface properties have been assumed on the basis of experimental test (basically tilt tests) performed at Aalto University (Sinnathamby et al. 2015).

The material parameters used in the interfaces are listed in Table 4-4.

Table 4-1. Hardening soil parameters.

Model Part	γ [kN/m³]	γ_{sat} [kN/m³]	E_{oed}^{ref} [MPa]	E_{50}^{ref} [MPa]	E_{ur}^{ref} [MPa]	v_{ur} [–]	m [–]	c' kPa	ϕ' [°]	ψ [°]	TCO [kPa]
Pellets	16.0	16.0	1.7	3.4	17	0.2	1	40	27	0	10

Table 4-2. Jointed Rock parameters.

Model Part	γ [kN/m³]	γ_{sat} [kN/m³]	E_1 [MPa]	v_1 [–]	E_2 [MPa]	v_2 [–]	G_2 [MPa]	c' kPa	ϕ' [°]	ψ [°]	TCO [kPa]
Blocks (continuum)	20.0	20.0	500	0.3	500	0.3	192.3	5	24	0	0
Jointset 1	$\alpha_1 = 90°$	$\alpha_2 = 0°$									
Jointset 2	$\alpha_1 = 90°$	$\alpha_2 = 90°$									

Table 4-3. Hoek-Brown parameters.

Model Part	γ [kN/m³]	γ_{sat} [kN/m³]	E [MPa]	v [–]	σ_{ci} [MPa]	m_i [–]	GSI [–]	D [–]	ψ [°]
Blocks (discrete)	20.0	20.0	500	0.3	1.6	10	98	0	0

Table 4-4. Interface parameters (Mohr-Coulomb and Hardening Soil).

Model Part Interface	E/ E_{oed}^{ref} [MPa]	E_{50}^{ref} [MPa]	E_{ur}^{ref} [MPa]	m [–]	v'/ v_{ur} [–]	c' kPa	φ' [°]	ψ [°]
Pellet-Buffer (MC)	10	–	–	–	0.2	1	5	0
Pellet-Block (MC)	10	–	–	–	0.2	1	24	0
Pellet-Rock (MC)	20	–	–	–	0.2	5	10	0
Buffer-Rock (LE)	0.001	–	–	–	0.0	–	–	–
Block-Block (HS)	1.5	3	9	0.5	0.2	1	24	0

4.3 Geometry of the model

Due to the geometrical irregularity and unevenness of the tunnel walls, it has been decided to include a close approximation of the real tunnel geometry, which was carefully reconstructed through laser scanning technique.

The geometry of the real tunnel has been simplified to take into account the geometry effects without compromising the feasibility of the calculation. Real geometry and simplified one are shown in Figure 4-1 whereas more detail of the geometry assumed for calculations is shown in Figure 4-2.

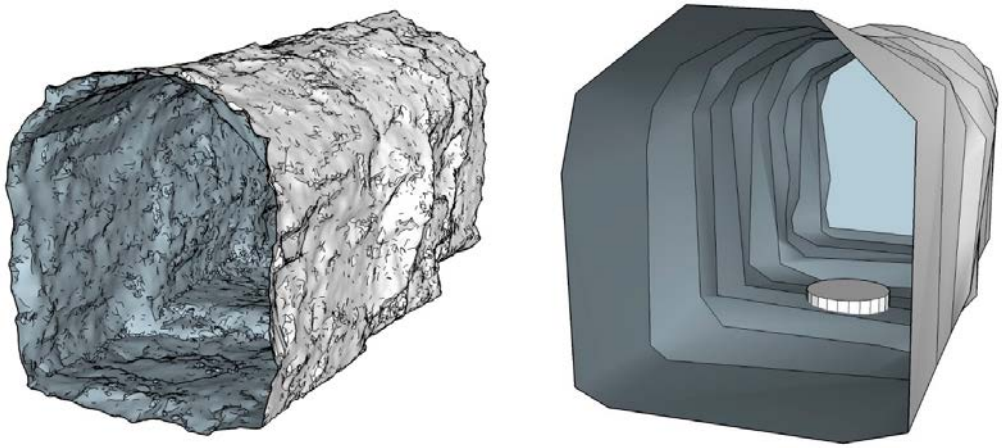

Figure 4-1. *(Left) 3D rendering of the tunnel geometry based on laser scanning and (right) simplified geometry for numerical analysis.*

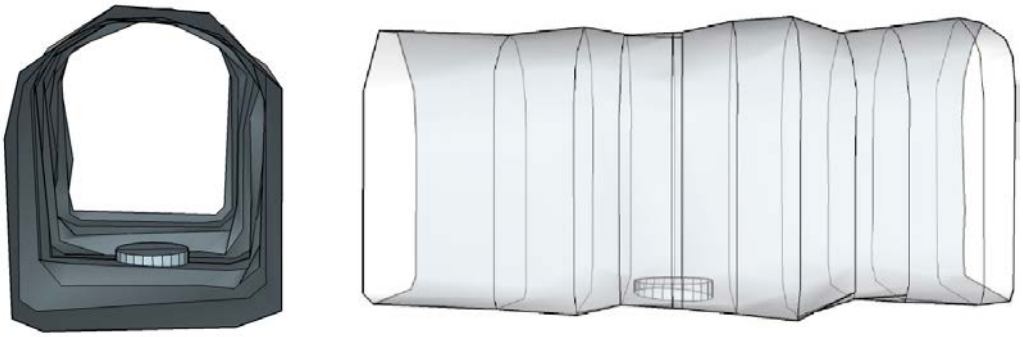

Figure 4-2. *Front view (left) and side view (right) of simplified deposition tunnel.*

Two distinct models have been defined, the purpose of the first preliminary model being the definition of the region interested by failure during loading. To this end, instead of modelling each block individually, only the horizontal layers have been explicitly included in the model, whereas the vertical joints in two orthogonal directions have been implicitly modelled by means of the Jointed Rock model.

This particular constitutive model has been described in previous Section 4-2. The geometry of the model is shown in Figure 4-3.

After identifying the region of interest, a second model has been set, with the difference that blocks and block-block interfaces have been fully modelled in the central region, whereas the blocks outside the region of main interest have been replaced by an equivalent continuum material (Figure 4-4) based on the above described Jointed Rock model. On doing so, the computational effort has been optimized by refining the mesh in correspondence of the loading plate and simplifying the model towards the boundaries without compromising the accuracy of the results.

The global size of the two models is identical, with a length of 12 m, 6 m width and 6 m height. The buffer block, as in reality, has a diameter of 1.65 m.

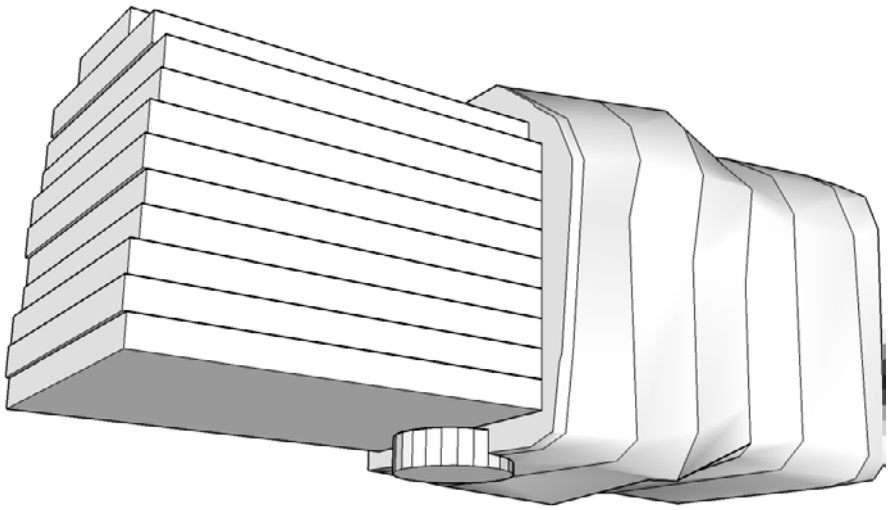

Figure 4-3. *Preliminary model.*

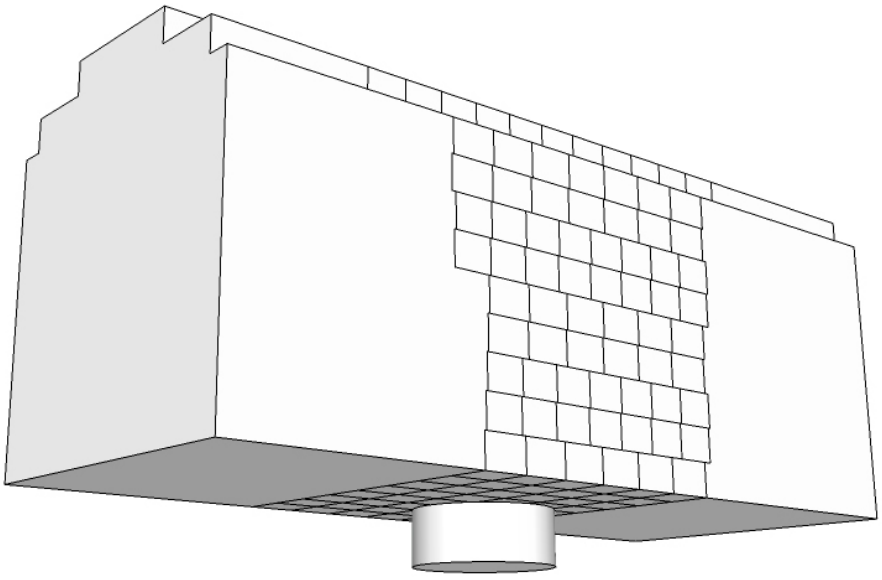

Figure 4-4. *Model with explicit blocks and continuum regions.*

4.4 Finite element model

The two geometries described in previous section have been meshed and included in two finite element models. The geometry of deposition tunnel is the same for the two geometries, as well as the bentonite pellets layer. The finite element mesh of the common parts is shown in Figure 4-5.

Horizontal and vertical displacements are prevented at the sides of the model with the exception of the buffer block at the centreline where a prescribed vertical heave has been applied.

Every calculation has been carried out in terms of effective stresses, with no generation of excess pore pressure and in perfectly dry conditions.

Interface elements have been assigned to every surface at the contact between different materials, i.e. rock, pellets, and blocks. The interface between the buffer block and the host rock has been set to linear elastic with zero stiffness (E = 0.001 kPa) to neglect any frictional contribution to the total force developed during loading as the pellets filling the 5 cm gap between buffer block and deposition hole were not compacted and therefore in a loose state.

The initial condition is of *whished-in-place* tunnel, blocks and pellets, as it is clear that the installation does not affect the calculation results.

The loading from beneath the buffer block is applied as prescribed vertical (upward) displacement in the first calculation phase.

4.4.1 Preliminary finite element model

The preliminary model with virtual blocks and homogenized layers consists in about 200 000 10-noded elements and 350 000 nodes, and the mesh of finite elements is shown in Figure 4-6 and Figure 4-7.

After applying the upward displacement to the buffer block the shape of plastic point distribution (Figure 4-8) and the relative shear stress (Figure 4-9) along the longitudinal section defines the region of interest, in which a more accurate modelling has been carried out by introducing explicit block geometry in the model. The variable “relative shear stress” defines a distance between the current stress state and the corresponding stress state at failure. A value of 1 means that the ultimate condition has been reached.

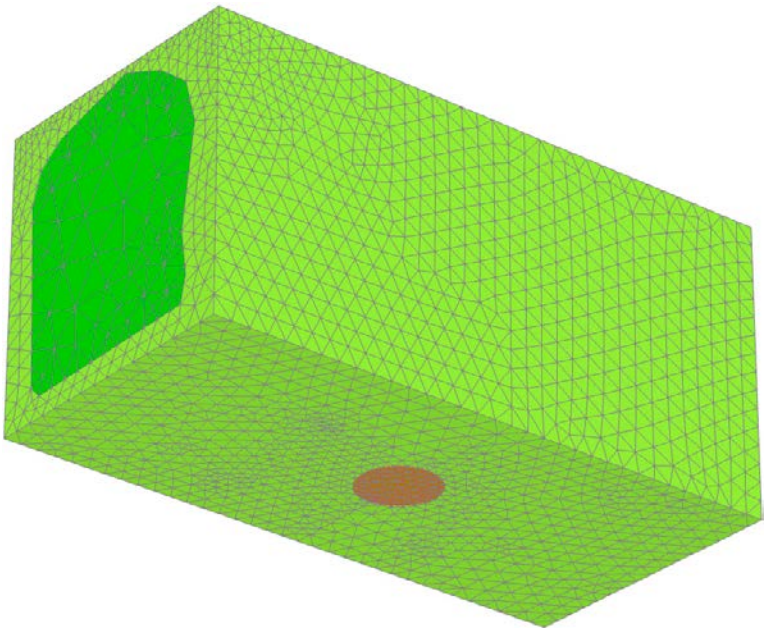

Figure 4-5. *3D Finite element model, bottom view. Prescribed displacement applied to the central disc with the same size as the buffer block.*

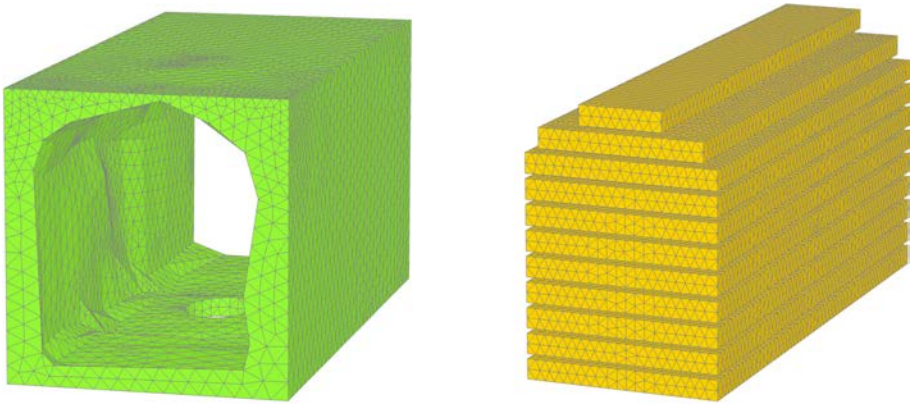

Figure 4-6. *(Left) Host rock and (right) exploded view of block layers.*

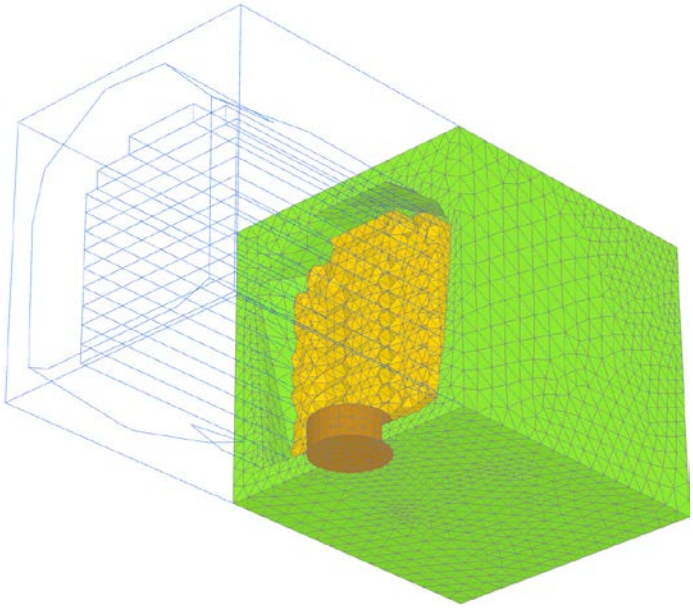

Figure 4-7. *Vertical section of the model at the loading plate. The gap between block layers and host rock is filled with a cluster of clay pellets.*

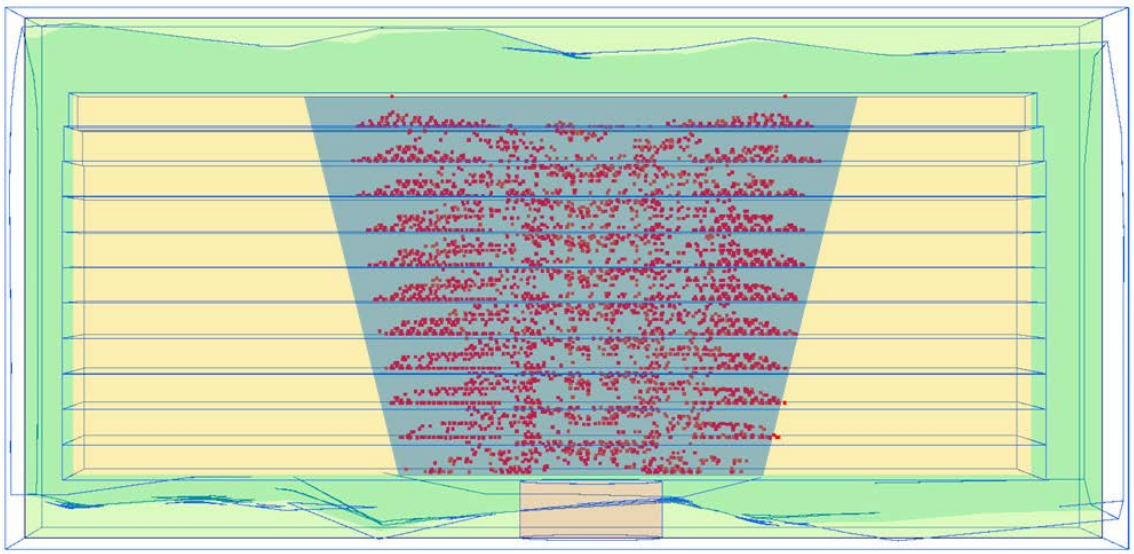

Figure 4-8. *Plastic points (in red) after loading and (shaded in grey) region of interest.*

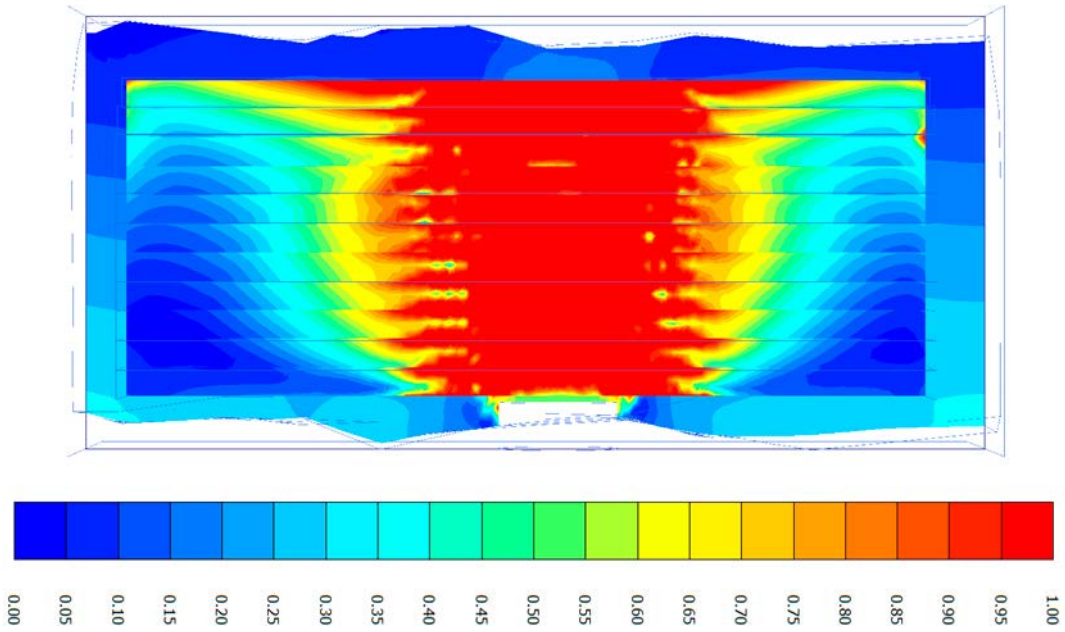

Figure 4-9. *Relative shear stress. A value of 1.00 (red) indicates a full mobilization of the shear strength, i.e. failure condition has been reached.*

4.4.2 Final finite element model

In the light of the results shown in previous chapters, it is clear that the central third of the model is mainly involved in the deformation process. Therefore, in the final model only the blocks populating that region have been explicitly modelled, whereas the outer regions have been modelled as continuum with the Jointed Rock constitutive model.

On the other hand, since the purpose of this study is the assessment of the importance of the failure of the blocks during loading, in addition to the global confirmation of constitutive assumptions and material parameters chosen for the block-block interface, the elastic-perfectly plastic Hoek-Brown model has been assumed for the discrete blocks.

Considering the large stress range reached during the test, the double-hardening Hardening Soil model has been selected for interface elements between blocks. The choice of a higher order model has been imposed by the need of a stress-dependent stiffness in addition to a failure criterion. In fact, assuming a constant stiffness parameter, as it is usually assumed in a crude Mohr-Coulomb model, would lead to less accurate results when the focus is on the evolution of the stress distribution up to failure.

The geometry used for simulating the Buffer swelling test is shown in Figure 4-10. In total 170 000 10-noded finite elements and 345 000 nodes have been used. The mesh has been densified in the central region, modelled with explicit blocks, whereas the solid clusters at the sides enabled a considerable simplification, thus reducing the calculation time.

After the initial phase where the model has been considered as *whished-in-place* in analogy with what assumed in the preliminary case, an upward displacement of 11 cm has been applied at the lower surface of the buffer block. In the following section the results are presented in terms of vertical displacement, block failure and major principal stresses.

The most obvious way to verify the capability of numerical model to capture the real behaviour of the system has been to compare the curve of the applied load versus the prescribed displacement. The numerical-experimental comparison in shown in Figure 4-11.

The initial part of the experimental curve shows a nearly straight line which turns into a convex line at a transition point of about 40 mm. It is assumed that the blocks undergo only minor breakage until that point, and the mechanical behaviour of the system is mainly controlled by the interfaces.

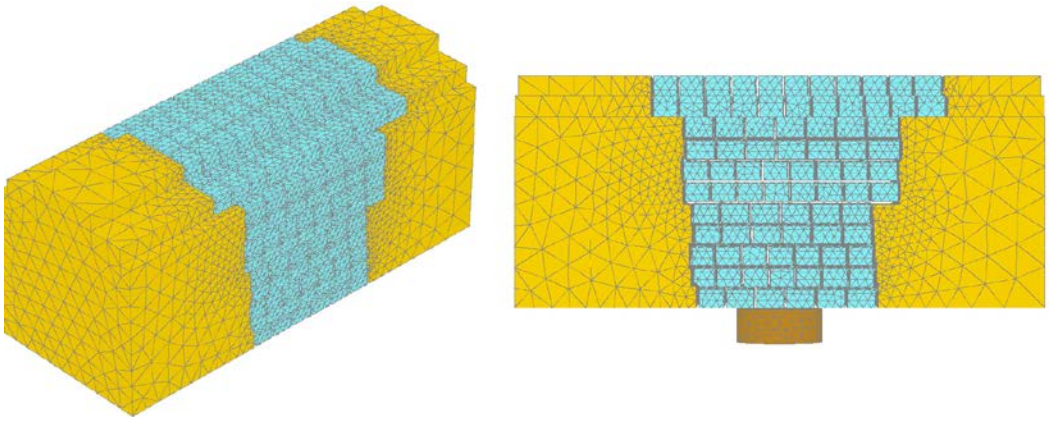

Figure 4-10. *Finite element mesh. (Left) Axonometric view and (right) side view.*

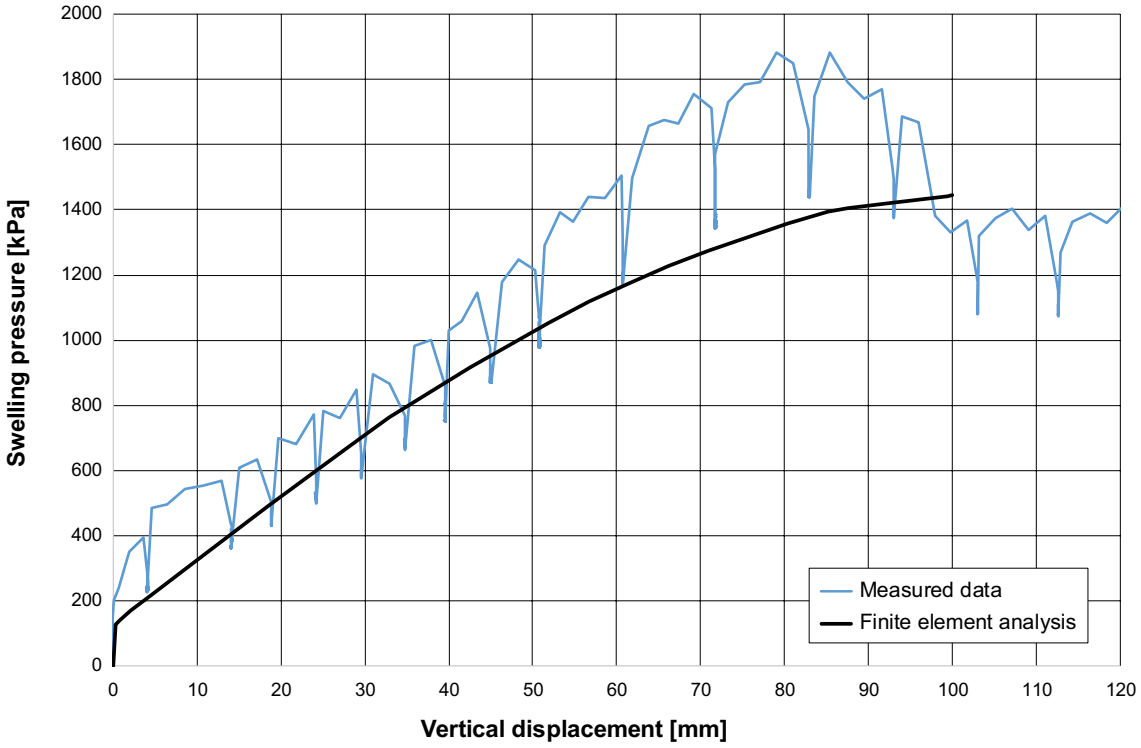

Figure 4-11. *Applied average stress on the loading plate versus prescribed vertical displacement. Experimental (light blue) and numerical (black) results.*

In the physical model the concavity, i.e. stiffening behaviour, can be explained as a progressive gap closure at the block interface level, whereas the change of concavity should be explained in the light of the onset of block cracking. This is captured by the numerical model which is not able to reproduce the stiffening effect as interface elements do not include initial gap closure, but the transition from concave to convex at about 40 mm in the experimental curve, corresponds to a change in the numerical curve from nearly straight to convex.

At a prescribed displacement of 11 cm a *plateau* has been reached in the numerical curve, which conventionally has been assumed as the end of the numerical simulation, as the model is not capable of modelling strain softening, for which a non-local formulation or equivalent approaches would be needed in order to avoid the well-known mesh dependency issue.

In the Buffer swelling test, in contrast, the test was continued well beyond the 11 cm, reaching a maximum displacement of 15 cm. However, the experimental curve shows an abrupt decrease in the applied force at a displacement value of about 8 cm, thus showing a softening behaviour probably due to the occurrence of a massive breakage of the blocks and consequent shear localization.

4.4.3 Failure of backfill blocks

As shown in Section 3.2 concerning the appearance of the block stack after loading, it is clear that the blocks in correspondence of the central section were intensively affected by a failure mechanism, with the exception of the topmost four layers. The top layers were indeed displaced without any apparent failure in the blocks. For the sake of readability, a picture of the stack of blocks after the test is shown in Figure 4-12.

The results of finite element analysis show a progressive failure which starts in proximity of the loading plate and propagates towards the top of the block stack. Figure 4-13 shows the progressive advancement of failed blocks during loading. The results are presented as the above decribed *relative shear* stress, and shear stress. A relative shear stress of 1 (in red) means failure. Comparing the last picture of Figure 4-13, which corresponds to the maximum displacement of 11 cm resembles very closely to the photo shown in Figure 4-12, which testimonies the good capability of the numerical model of capturing the transfer mechanism through the failed blocks.

As in reality, the two columns of blocks on each side of the stack and the four topmost rows are still intact after loading.

Figure 4-14 shows the evolution of deviatoric stress (defined the same as the ABAQUS' von Mises q stress) with the advancement of the loading plate.

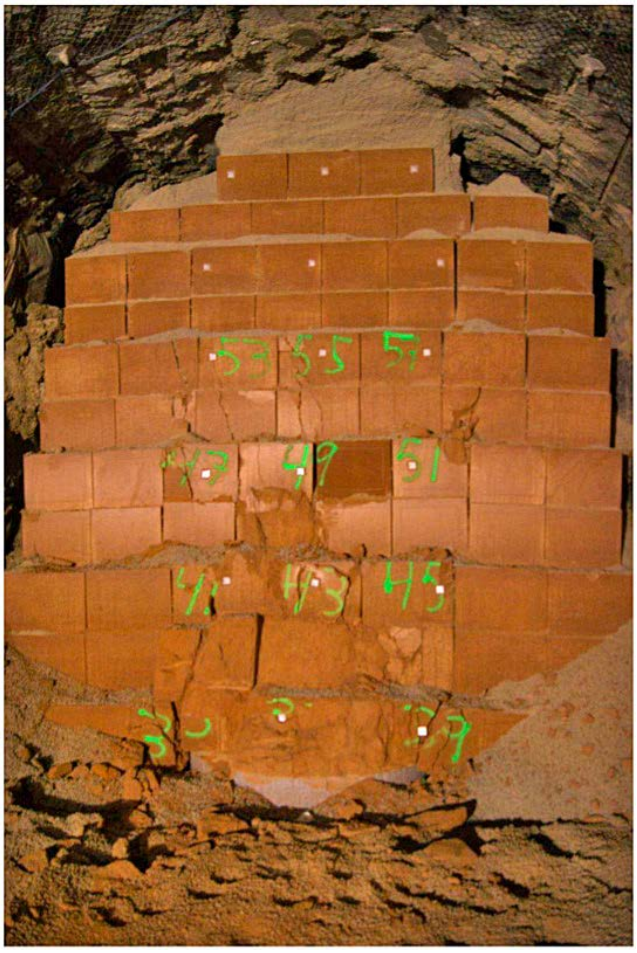

Figure 4-12. *Photo Post-mortem of the stack of blocks.*

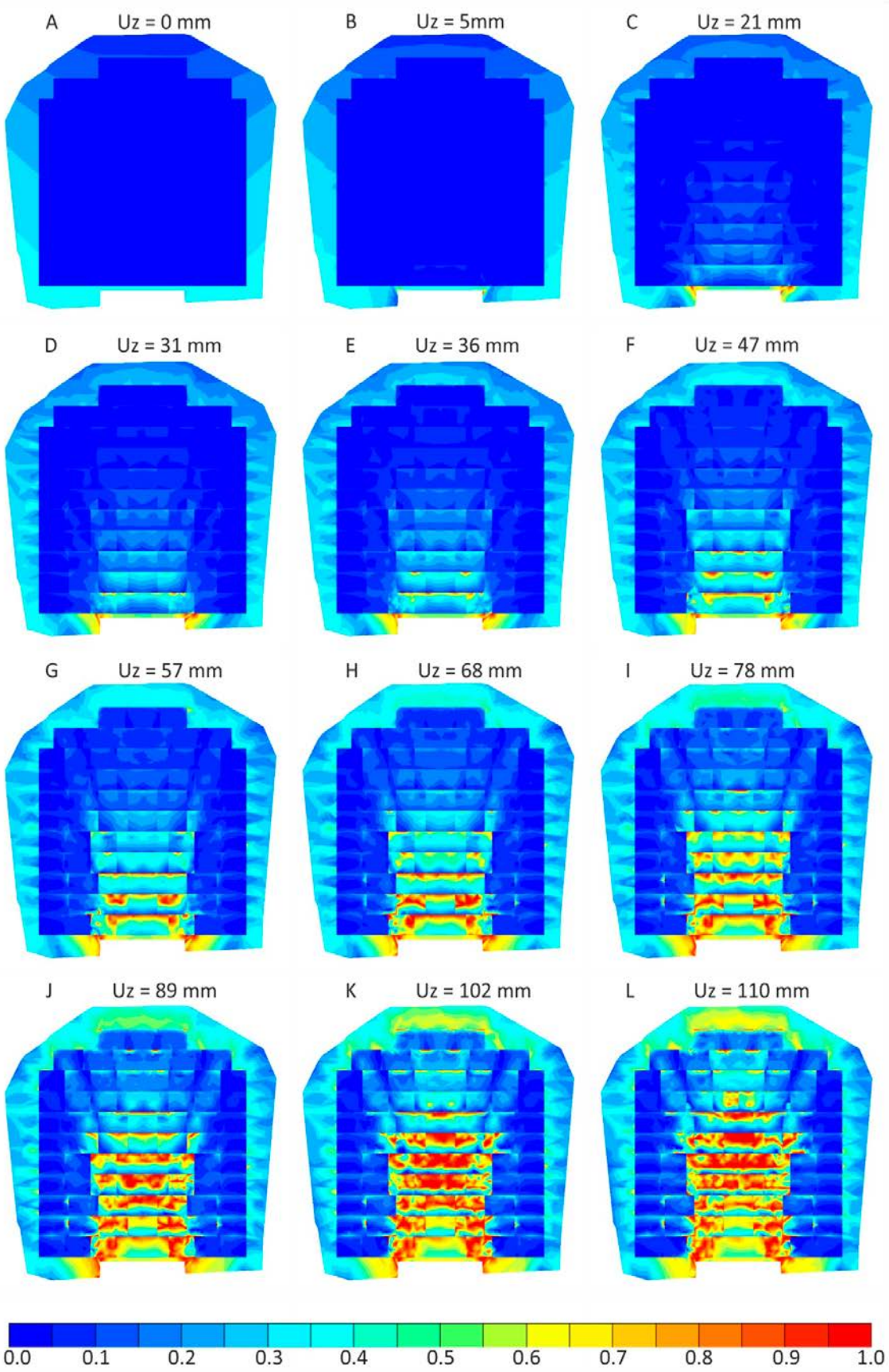

Figure 4-13. *Relative shear stress (from left to right and top to bottom and, upward displacement from 0 to 110 mm), location of each stage on load-displacement curve and with close-up on 110 mm stage.*

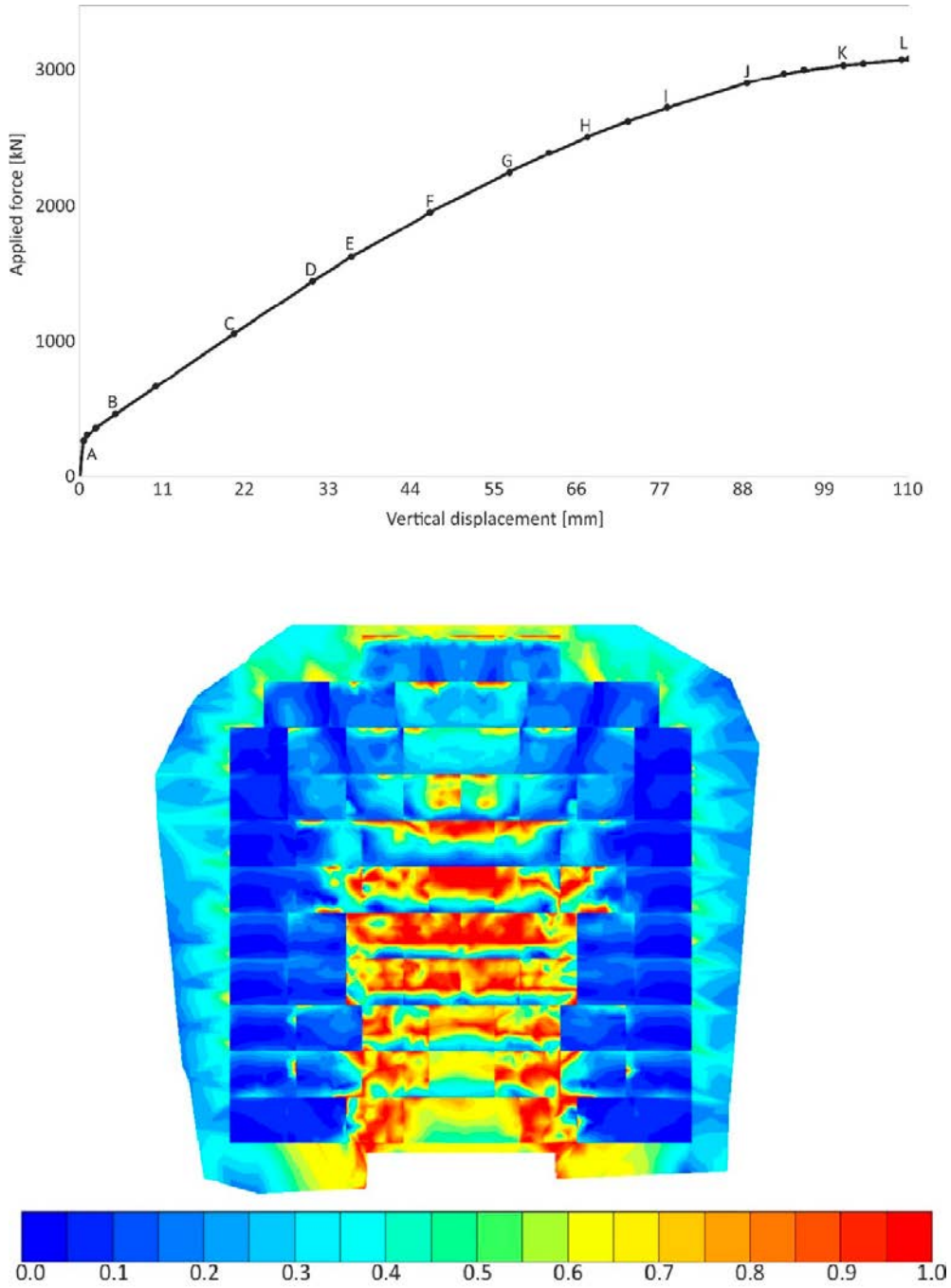

Figure 4-13. *Continued.*

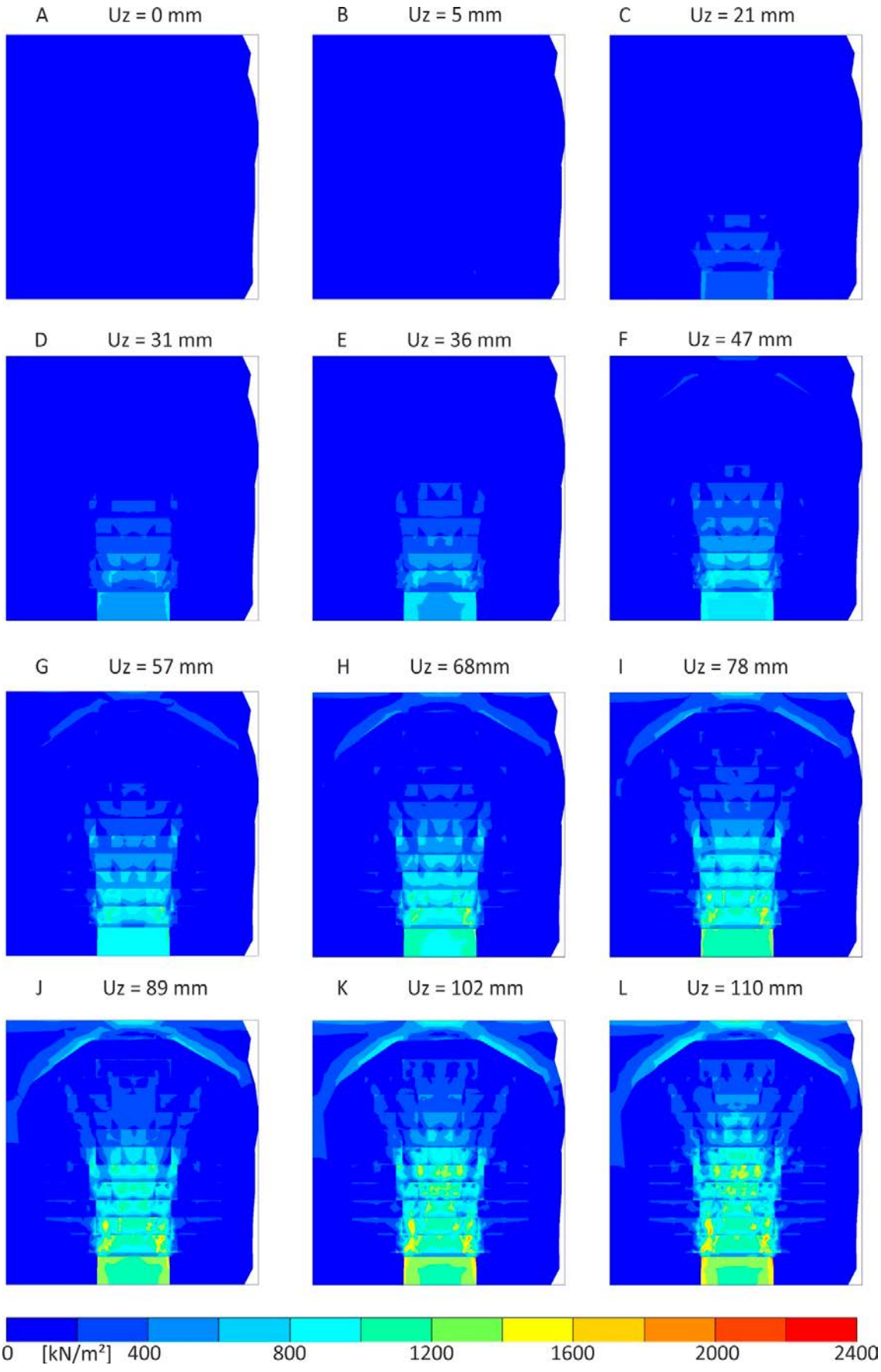

Figure 4-14. *Deviatoric stress (from left to right and top to bottom and, upward displacement from 0 to 110 mm), location of each stage on load-displacement curve and with close-up on 110 mm stage.*

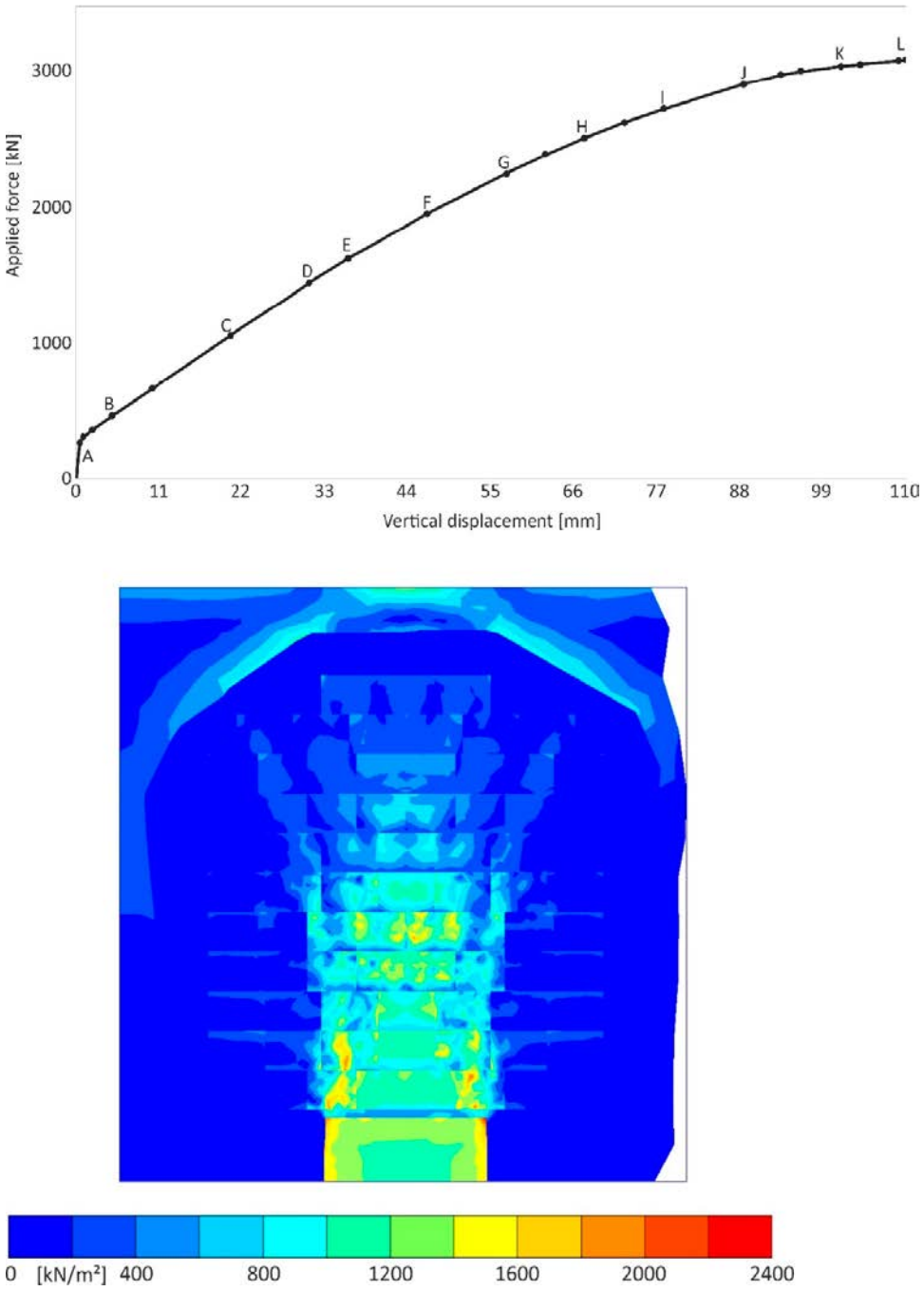

Figure 4-14. *Continued.*

4.4.4 Vertical displacement

The vertical movements in the backfill block stack occurring during loading were measured at the end of the test, and can be compared to the corresponding values obtained via numerical analysis. In Figure 4-15 the output of vertical displacement after loading shows a maximum heave of 93 mm at the base of the stack in correspondence of the buffer block. The in situ measurements after the test showed a maximum displacement of 114 mm (Sandén et al. 2017). The difference between measurement and numerical analysis is due to the different value of vertical displacement applied in the numerical test, which has been set to 11 cm in contrast to the 15 cm reached in the test. The reason for that assumption is in the very large deformation occurring in proximity of the buffer block, which made the calculation unstable.

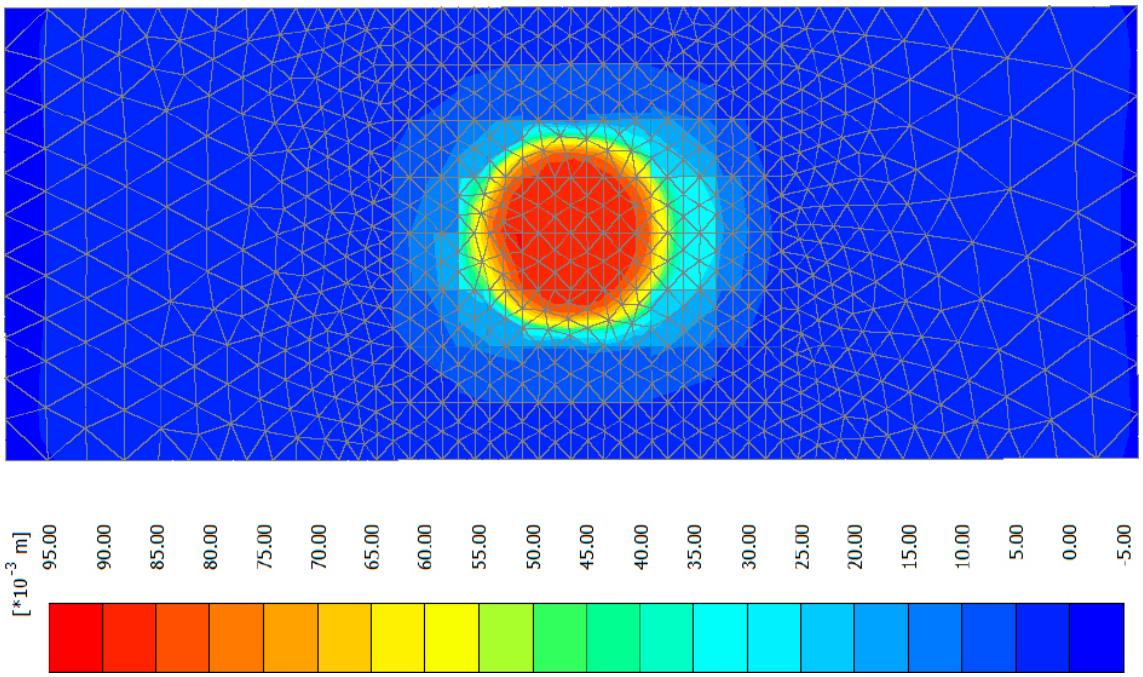

Figure 4-15. *Vertical displacement at the base of block stack (from below) at a plate displacement of 110 mm. Maximum heave of 93 mm.*

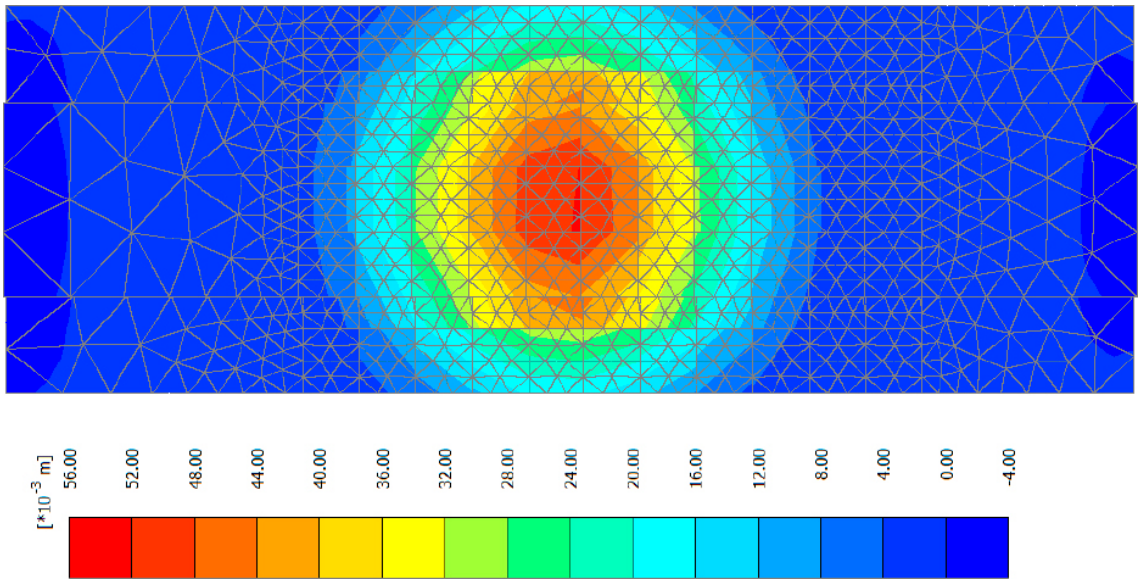

Figure 4-16. *Vertical displacement at the top of block stack (from above) at a plate displacement of 110 mm. Maximum heave of 53 mm.*

On the other hand, at the top of backfill block stack, a slightly overestimated value was recorded at the top of the block stack, being the maximum heave from numerical analysis 53 mm versus the measured 40 mm (Figure 4-16). No doubt, applying a displacement of 15 cm instead of the current 11 cm would lead to a further increase of this value, thus showing a general increase of the stack heave, in agreement with the measured values showing a maximum heave of about 60 mm in the topmost three rows (Figure 4-27 in Sandén et al. 2017).

As for the distribution of the vertical displacements in correspondence of the loading plate, from numerical analysis appears that about 55 % of the total compression occurs in the pellets, whereas the measurement reveals that 50 % is more likely value. Considering the uncertainties in the geometry of the rock roof, and since there is a large variability of the readings depending on the exact position where the measurement occurs, the slight discrepancy is judged not relevant.

Furthermore, considering that the total vertical displacement applied in the model has been 110 mm in contrast to the real 150 mm, and in the light of the massive breakage that occurred in the lowest part of the block stack, the remaining 4 cm would probably concentrate more in the plastic region, thus increasing the proportion of vertical displacements in the stack as opposed to the pellet layers.

4.4.5 Major principal stress and interface normal stress

Pressure cells installed at the tunnel crown showed a pressure in excess of 300 kPa, value that should compared to the normal stress measured at the interface between rock roof and pellet layer. The corresponding plot is shown in Figure 4-17. At the crown the peak value obtained in numerical analysis is slightly above 300 kPa, decreasing to about 250 kPa moving towards the walls. After reaching the walls the interface normal stress decreases to values around 40 kPa. The stress distribution in the cross section of Figure 4-17 is in good agreement with the values measured by pressure cells 1, 3 and 4 by the end of test.

In Figure 4-18 is depicted the evolution of major principal stress, which is practically coincident with vertical Cartesian stress in correspondence of buffer block. The results are only limited to the pellet layer, in a vertical section at the centreline of the buffer block.

The inner part of each plot is a front view of the sides of the model, therefore not significant for the present analysis. It is clearly visible how during loading the stress increases at the crown, from nearly zero (blue) to the maximum value of 200 kPa at the end of loading.

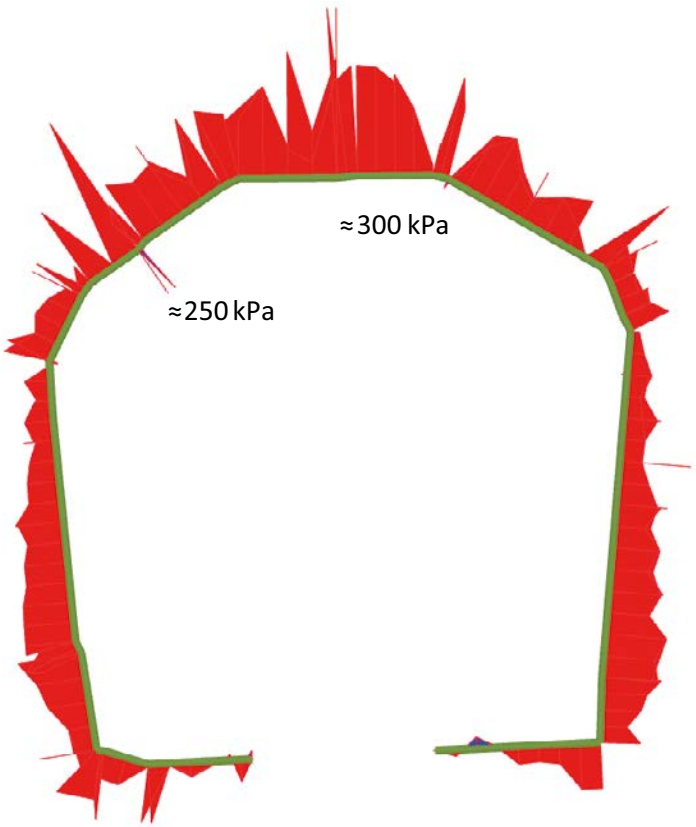

Figure 4-17. *Effective normal interface stress at a plate displacement of 110 mm. Cross section at the centreline of buffer block.*

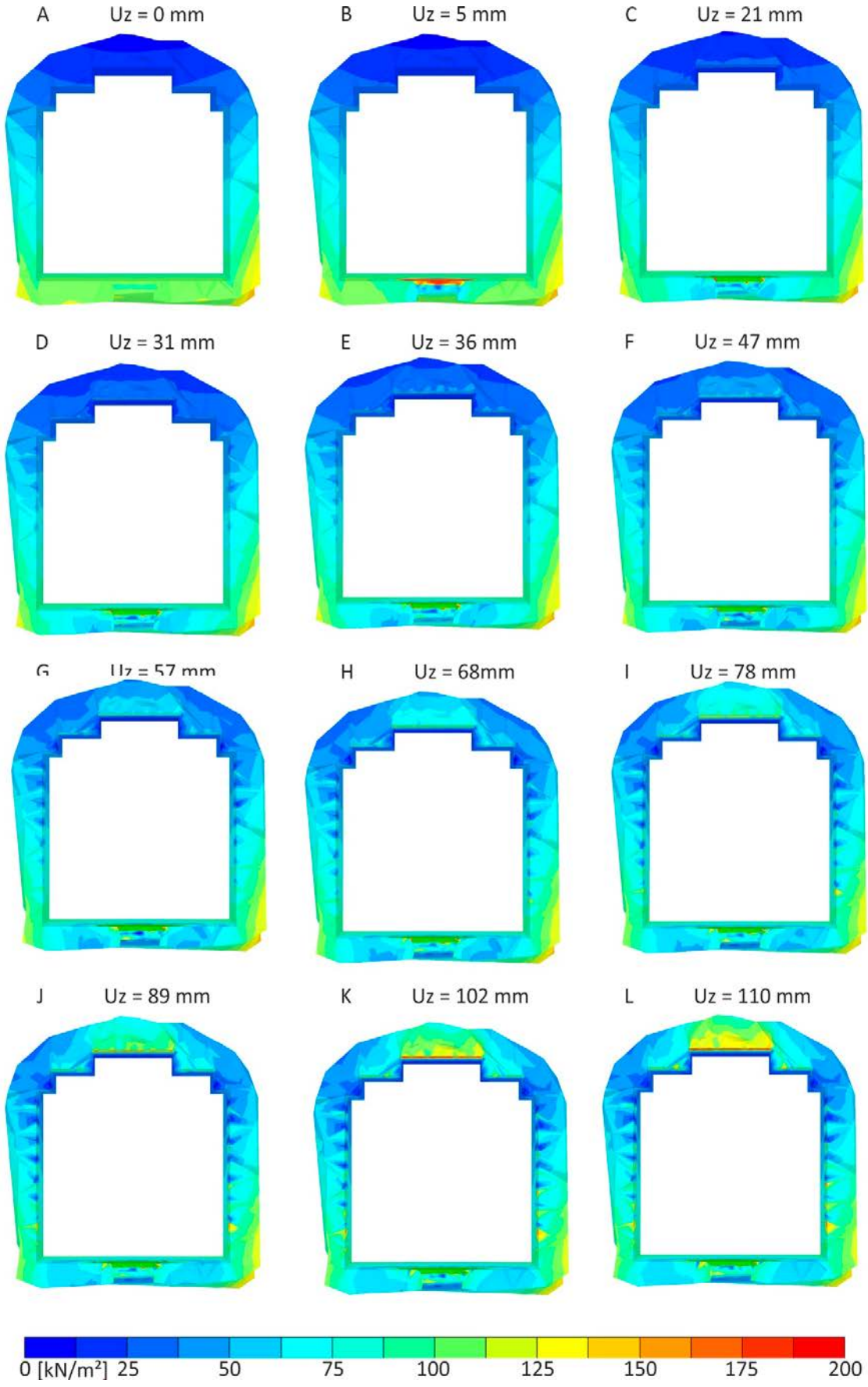

Figure 4-18. *Major principal stress in the pellets during loading (from left to right and top to bottom and, upward displacement from 0 to 11 cm), location of each stage on load-displacement curve and with close-up on 110 mm stage.*

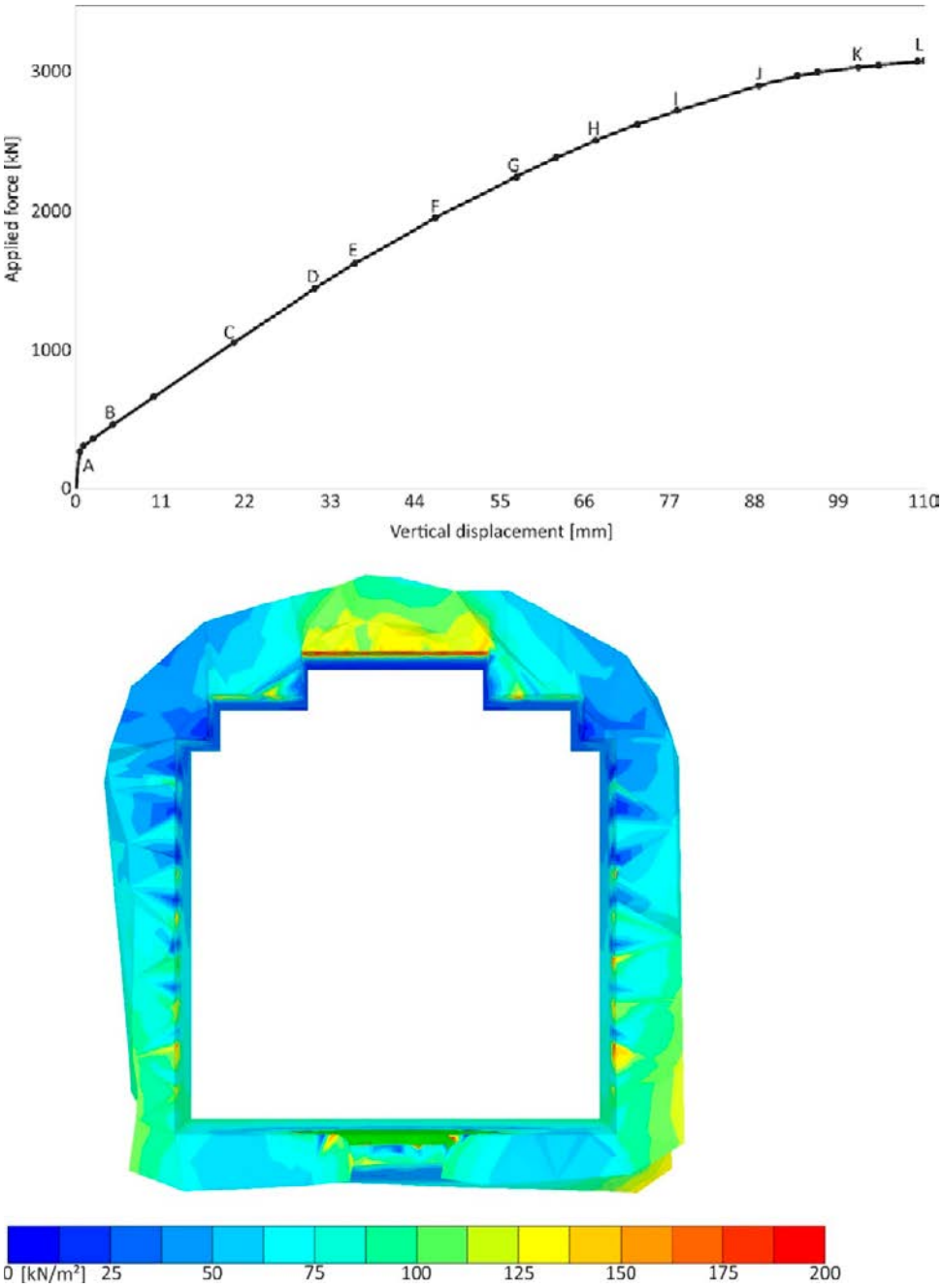

Figure 4-18. *Continued.*

4.4.6 Major principal stress in pellet fill

The distribution of the principal stress increase in correspondence of buffer block confirms that the central third of the model is involved in the main deformation process, which is also verified by the decreasing number of broken (or heavily displaced) blocks getting away from the central part of the test. The colourmap of major principal stress in pellet layer is shown in Figure 4-19 in its evolution throughout the test.

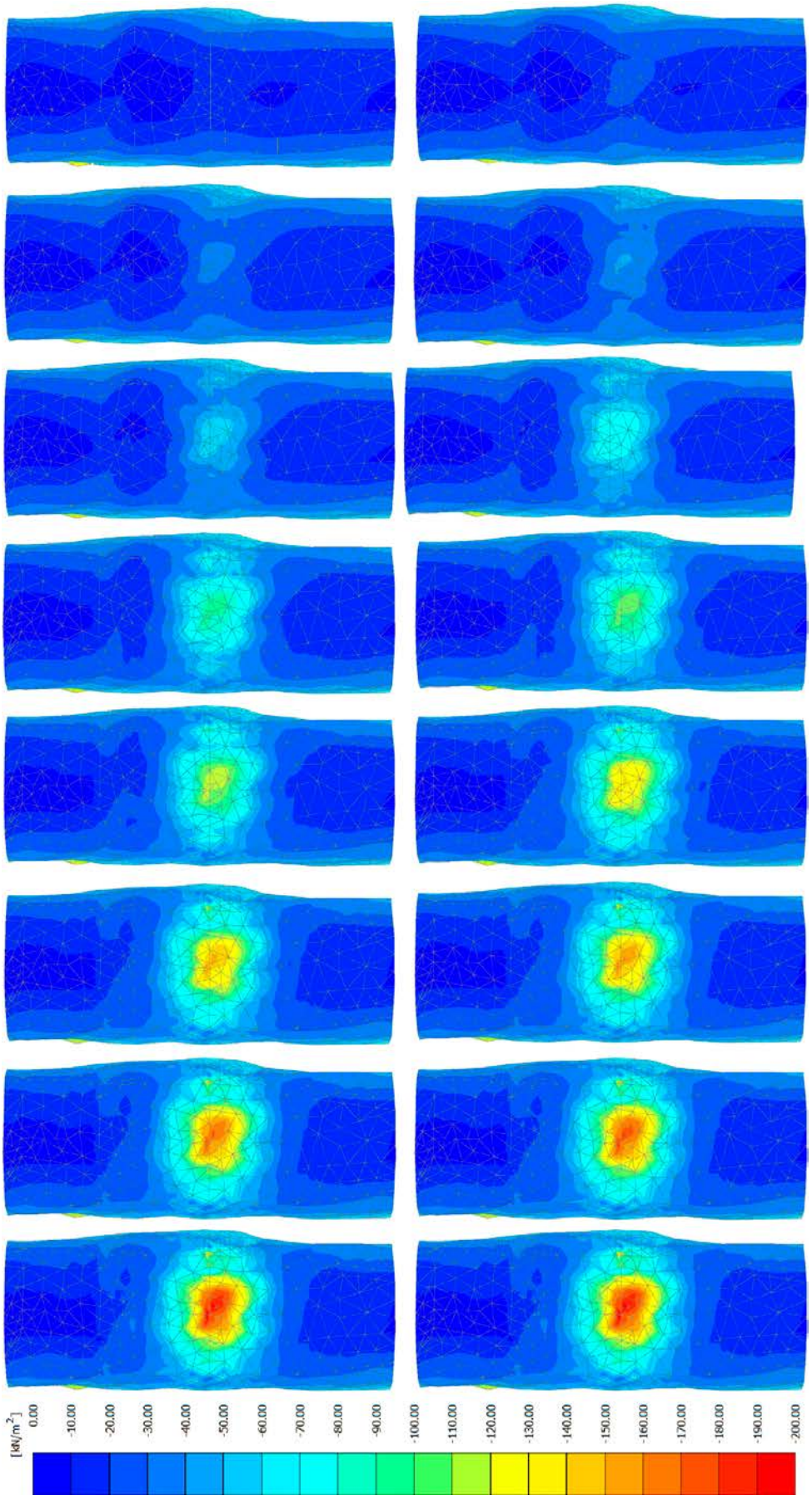

Figure 4-19. *Major principal stress on top surface of bentonite pellet layer (from left to right and top to bottom and, upward displacement from 0 to 11 cm).*

4.5 Discussion of the results with PLAXIS calculations

The numerical modelling of Buffer swelling test has been carried out by taking into account the uniaxial unconfined strength value which was determined through a series of laboratory tests. The block strength has been then used to identify the parameters of a well-known failure envelope, the so-called Hoek-Brown criterion incorporated in the elastic-perfectly plastic name that goes under the same name and implemented in the standard library of PLAXIS code.

It has been assumed that the mechanical behaviour of the blocks is equivalent to a fairly undisturbed, intact argillaceous rock, with the stiffness properties which were determined by previous laboratory tests.

The mechanical behaviour of block-block interface has been assumed as elastoplastic with stress-dependent stiffness based on previous modelling experience. The identification of strength parameters was based on and further laboratory tests performed at Aalto University.

The host rock has been assumed as a boundary condition, i.e. a very stiff linear elastic material, whereas the clay pellets have been modelled with the aforementioned Hardening Soil model. All the remaining interfaces between different material have been modelled as linear elastic-perfectly plastic with parameters identified on the basis of previous studies.

The global load-displacement curve shows that the numerical model is able to reproduce the in situ test reasonably well, both from the qualitative and quantitative point of view. The first part of the force-displacement curve shows a mainly linear behaviour, followed by a convex portion starting at about 40 mm until a horizontal asymptote is reached.

The propagation of block failure from the bottom row proceeds towards the roof as the loading advances, and it does not penetrate through the whole stack even when the ultimate load has been reached.

Only blocks belonging to the central columns of the stack failed during testing, whilst the outer ones where only affected by upward or lateral displacements.

The global displacement field is compatible and in line with the measurements.

The average interface pressure at the roof is close to the measured values, as well as at the intersection between roof and walls. Right below the intersection, the normal pressure drops to smaller values, all that in agreement with the measurements.

For all the above, it is clear that the numerical model is capturing the main features observed in the experiment, thus confirming the validity of constitutive assumptions and material parameters assumed for the analysis.

5 Discussion

5.1 Differences between the Abaqus and PLAXIS calculations

Within the common framework of the Finite Element method, two different commercial software, namely Abaqus and PLAXIS, have been used for modelling the evolution of some THM processes that may take place in the buffer and backfill in the Swedish and Finnish underground repositories of spent nuclear fuel. The present report presents the results where these codes have been used for modelling the consequences of having a wet buffer that swells against a completely dry backfill. The modelling results have been compared to measured results of a full scale test in Äspö HRL.

Although the global approach of these codes in resolving the system of governing equations is basically the same, there are some differences, which are mainly affecting the results obtained. In addition the geometrical element models and the material models of the blocks and the joints between the blocks have been different. In this section, the main differences are analyzed and discussed, along with the check of their consequences on the results.

Geometry

Regarding the geometry, a tunnel with constant section has been modelled in Abaqus, whereas a close approximation of the as-built tunnel has been considered in PLAXIS. As a consequence, the thickness of the pellet floor is varying outside the load plate, which influences the strain distribution around the loading region, but not the force – displacement relation. In the Abaqus model the thickness of the pellet filling is 80 mm. In the PLAXIS model the thickness ranges between 30 mm and 600 mm and is 80 mm between the buffer block and the backfill block stack. The influence of this difference is regarded to be small since the compression of the backfill takes place above the simulated buffer block and does not involve the pellets outside the buffer block.

In Abaqus the entire block configuration has been modelled while in PLAXIS only the central third has been included with as separate blocks. This difference is considered to be of very little importance since the outer parts are almost unaffected.

Pellets

The constitutive model chosen for the pellet region is for the Abaqus model linear elastic with Drucker-Prager failure envelope. In the PLAXIS model an elastoplastic model with double hardening surface, namely the Hardening Soil model was chosen. A Mohr-Coulomb failure envelope is included in the Hardening Soil model, thus limiting the admissible stress states. The stiffness is in this model governed by three distinct stiffness moduli in oedometric compression, shear at 50% of maximum deviator stress, and unloading/reloading.

Considering the high stress gradient around the loading region and the stress range varying from 100 kPa to 1 800 kPa, it is of course more relevant to have an elastoplastic nonlinear model than a linear elastic. However, for the purpose of the present modelling the linear relation is judged to be acceptable since it deviates not more than 4 % from the actual measured stress-strain relation.

The conclusion of the comparison is that the elastoplastic model of PLAXIS of course can be made a better model for modelling general stress-strain behaviors of pellet fill. However, this requires a careful calibration of all parameters in order to show that it behaves as intended. But it is not the purpose of the report to judge which model gives the best results. Both models are acceptable for the purpose of evaluation the Buffer swelling test.

Joints

In the Abaqus model contact surfaces are used to model the joints between the blocks while the PLAXIS model uses interface elements.

The differences in the joint models are analyzed in detail in Table 5-1.

Table 5-1. Joint models.

Abaqus	PLAXIS
Contact surface behaviour • Non-linear stress-strain relation. Sliding is modelled with ϕ = 20º; • An initial virtual gap of 4 mm is assumed between block surfaces; • Full closure of virtual joints at a normal pressure of 10 MPa; • User-defined non-linear normal stress-displacement curve	*Interface elements* • 2D finite elements with 8 node-pairs and 9 integration points; • Normal and tangential elastic stiffness, which linearly depend on the virtual thickness and the normal and shear stress, respectively; • Mohr-Coulomb failure envelope, with ϕ = 24º and c' = 1 kPa.

It is difficult to compare the two models since they are so different. In order to do that the stress-compression relation at normal stress increase for the PLAXIS model must be derived and compared to the relation shown in Figure 3-1, which is used in the Abaqus model.

Blocks

The models of the block materials are described in Table 5-2.

Table 5-2. Block material models.

Abaqus	PLAXIS
Elastic elements • Linear elastic; • No failure included	*Interface elements* • Elastic-perfectly plastic; • Hoek-Brown stress-dependent failure envelope; • Uniaxial compression strength limited to σ_{ci} = 1 600 MPa

The material models of the blocks also differ very much. The idea of the Abaqus model was not to model cracking since the calculation was meant to be identical to previous calculations done for designing the backfill in order to evaluate those calculations and cracking is envisaged to not be allowed to take place in a real repository due to the resulting large upwards displacements. So the model was very simple linear elastic.

In the PLAXIS calculations the material model of the blocks was designed to reproduce more closely the real mechanical behavior and include the failure of the blocks. So this model was elastoplastic with a failure envelope and a maximum compression strength. However, the failure of the blocks does not simulate cracking but instead plastic deformation.

5.2 Evaluation of results

Both Finite Element models are able to capture the upward force associated in correspondence of the heave that corresponds to the peak value. Neither of the models is able to follow the post-peak behaviour.

However, the different approach followed in modelling the mechanical behaviour of the blocks lead with Abaqus to a straight linear response of the system throughout loading, whereas in PLAXIS analysis the load-displacement curve clearly defines the ultimate swelling pressure the backfill is able to withstand as a whole.

In Figure 5-1 the results from the two models are compared together with the measured results. For PLAXIS both the modelled results with blocks that can plasticize and results were the plastication is shut off are shown. The notches in the measured results are caused by the loading technique. The load was applied stepwise, which resulted in an immediate response and then creep caused by stress relaxation until the next step was applied.

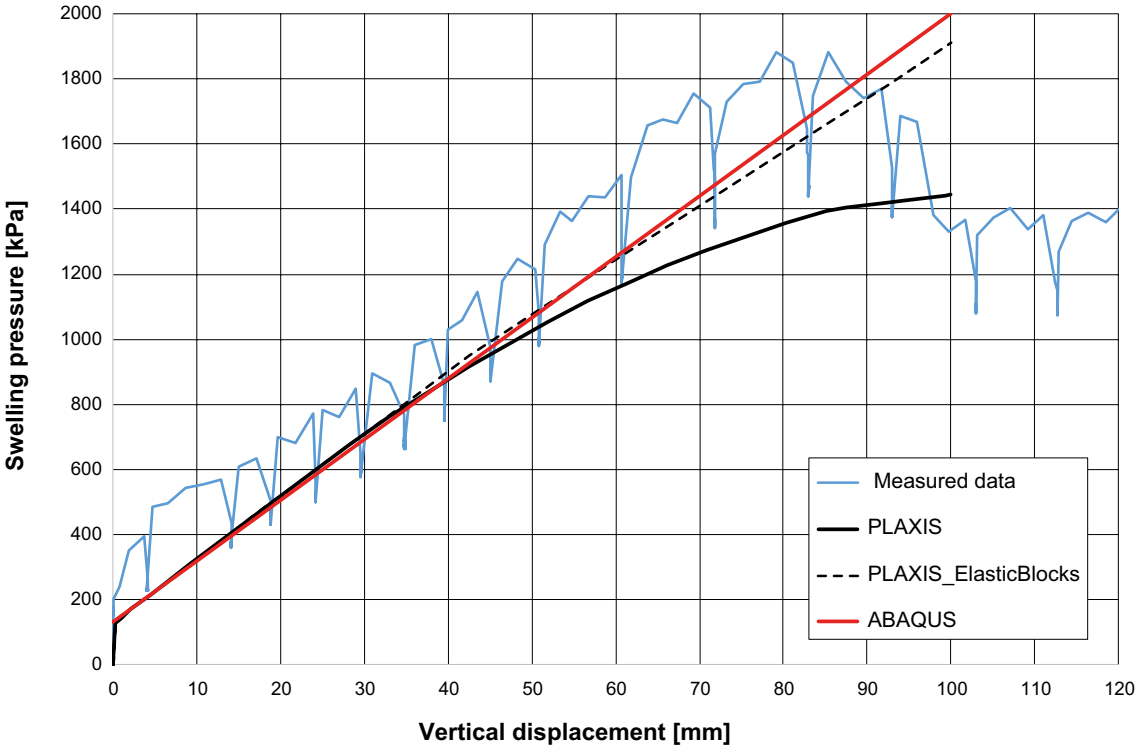

Figure 5-1. *Comparison of measured and modelled relation between vertical displacement of the plate and applied normal stress on the plate. The black solid and dashed lines are the PLAXIS results and the red line corresponds to the Abaqus results.*

The two models with elastic blocks yield very similar results with practically straight line relations, which also agree very well with the measured results, up to 70–80 mm displacement. At higher displacements the modelled relations differ from the measured due to the cracking of the blocks. The PLAXIS model with blocks that may plasticize yields a relation that deviates from the straight line due to cracking occurring in some blocks as shown in Figure 4-12.

The measured relation has a very small concave deviation from the straight line, probably mainly caused by the stiffening of the pellet filling and the joints between the backfill blocks. The stiffening of the pellet filling was not included in the Abaqus model so the concave deviation is not modelled. The stiffening is meant to be included in the PLAXIS model but it does not clearly show in the stress relation, probably due to the limited thickness of the hardening region.

The experimental data show that between 4 and 5 cm there is a small change from a concave relation to a convex relation, which may indicate very local cracking in the backfill blocks close to the buffer block. However, the notches in the measured data makes this evaluation uncertain. Between 7 and 8 cm there seems to be a massive failure in many backfill blocks with pervading fractures that lead to a peak value in stress with consequent stress decrease.

The Abaqus model thus seems to very well capture the behavior of a system with blocks that have so high strength that they do not crack. The model should though be improved by including the stiffening of the pellet filling with increased stress. The model is of course completely unable to capture the behavior of blocks that crack during loading.

The PLAXIS model shows the effect of block plasticity after 40 mm displacement by deviating from the straight line and reaching close to a maximum after 100 mm displacement. In the model were the plasticity of the blocks had been excluded the results up to 100 mm form almost a straight line in agreement with the Abaqus model. It seems that the plastic model underestimates the maximum stress. This could be caused by the fact that local plasticity of blocks deforms the block even though the plastic zone does not penetrate the entire block, while cracking only deforms the blocks if the cracks go through the blocks.

5.3 Validity of the models

As demonstrated in Sections 3 and 4, though based on different assumptions, both Abaqus and PLAXIS models are able to capture the relevant behaviour of the backfill up to failure of the bentonite blocks as installed in Äspö HRL test site, which has been taken as reference for the validation of the Finite Element models.

The purpose of the two models has been a little different. The Abaqus model has aimed at studying the process up to failure of the blocks with the argument that blocks with much higher strength than the blocks used can be produced, while the PLAXIS model was also done with the purpose to study the effect of block plasticity.

It is not completely obvious when cracking has started and what effect it may have had. The PLAXIS analysis indicates that plasticity and possible cracking may have stated already after 30–40 mm displacement, but since the onset of plastic strains has been rather local in the blocks at that time and not all through until after 70–80 mm displacement, it may not have given consequences for the resistance of the backfill against buffer swelling until that displacement. The good agreement between both the Abaqus model and the elastic PLAXIS model and the measured results up to 80 mm displacement support that conclusion.

An overall conclusion of the modelling capability is that both codes and models are capable of predicting the resistance to upwards swelling of a dry backfill if no extensive cracking of the blocks occur. It is not obvious that the effect of cracking can be well modelled with an elastoplastic material model of the blocks since there are differences between cracking and plastic strains but it seems that the maximum restraining pressure against upwards swelling is captured and it seems, in this particular case, to be close to the uniaxial compression strength of the blocks.

As for the block-block interaction, PLAXIS offers interface elements which are not particularly suited to model contact problems; however the equivalent stress-dependent stiffness is reasonably effective in capturing the mechanical behaviour of the joints.

In both models, the same parameter set and modelling as used in previous calculations was applied to the modelling of this test case, and the correctness of the assumptions is confirmed by comparison to measured stresses and displacements. In PLAXIS model the only element of novelty has been the plasticity Hoek-Brown model for the blocks, whose mechanical parameters have been calibrated through the unconfined uniaxial compression laboratory tests, whereas the empirical parameters have been identified as typical values and then fine-tuned via back analysis.

Therefore, from the overall performance it seems obvious that the two modelling approaches and the selected parameter sets can be considered suitable to model buffer/backfill interaction problems although some improvements can be done.

References

SKB's (Svensk Kärnbränslehantering AB) publications can be found at www.skb.com/publications.

Andersson L, Sandén T, 2012. Optimization of backfill pellet properties. ÅSKAR DP2. Laboratory tests. SKB R-12-18, Svensk Kärnbränslehantering AB.

Arvidsson A, Josefsson P, Eriksson P, Sanden T, Ojala M, 2015. System design of backfill. Project results. SKB TR-14-20, Svensk Kärnbränslehantering AB.

Börgesson L, Hernelind J, 2009. Mechanical interaction buffer/backfill. Finite element calculations of the upward swelling of the buffer against both dry and saturated backfill. SKB R-09-42, Svensk Kärnbränslehantering AB.

Börgesson L, Hernelind J, 2014. Modelling of the mechanical interaction between the buffer and the backfill in a KBS-3V repository. Updated design of backfill and deposition hole. SKB R-14-21, Svensk Kärnbränslehantering AB.

Börgesson L, Hernelind J, 2017. Modelling of the mechanical interaction between the buffer and the backfill in KBS-3V. Modelling results 2015. SKB TR-16-08, Svensk Kärnbränslehantering AB.

Börgesson L, Johannesson L-E, 2006. Consequences of upwards swelling from a wet deposition hole into a dry tunnel with backfill made of blocks. A preliminary study. SKB TR-06-12, Svensk Kärnbränslehantering AB.

Börgesson L, Johannesson L-E, Sandén T, Hernelind J, 1995. Modelling of the physical behaviour of water saturated clay barriers. Laboratory tests, material models and finite element application. SKB TR 95-20, Svensk Kärnbränslehantering AB.

Glamheden R, Fälth B, Jacobsson L, Harrström J, Berglund J , Bergkvist L, 2010. Counterforce applied to prevent spalling. SKB TR-10-37, Svensk Kärnbränslehantering AB.

Johannesson L-E, 2008. Backfilling and closure of the deep repository. Phase 3 – pilot tests to verify engineering feasibility. Geotechnical investigations made on unsaturated backfill materials. SKB R-08-131, Svensk Kärnbränslehantering AB.

Keto P (ed), Hassan Md M, Karttunen P, Kiviranta L, Kumpulainen S, Korkiala-Tanttu L, Koskinen V, Jalonen T, Koho P, Sievänen U, 2013. Backfill Production Line 2012. Design, production and intial state of the deposition tunnel backfill and plug. Posiva 2012-18, Posiva Oy, Finland.

Leoni M, 2013. 2D and 3D finite element analysis of buffer–backfill interaction. Posiva 2012-25, Posiva Oy, Finland.

Posiva, 2012. Safety case for the disposal of spent nuclear fuel at Olkiluoto – Design basis 2012. Posiva 2012-03, Posiva Oy, Finland.

Sandén T, Olsson S, Andersson L, Dueck A, Jensen V, Hansen E, Jonsson A, 2014. Investigation of backfill candidate materials. SKB R-13-08, Svensk Kärnbränslehantering AB.

Sandén T, Börgesson L, Nilsson U, Dueck A, 2017. Full scale buffer swelling test at dry backfill conditions in Äspö HRL. In situ test and related laboratory tests. SKB TR-16-07, Svensk Kärnbränslehantering AB.

Schanz T, Vermeer P A, Bonnier P G, 1999. The hardening soil model: formulation and verification. In Brinkgreve R B J (ed). Beyond 2000 in computational geotechnics: 10 years of PLAXIS International : proceedings of the International symposium Beyond 2000 in computational geotechnics, Amsterdam, 18–20 March 1999. Rotterdam: Balkema, 281–290.

Sinnathamby G, Korkiala-Tanttu L, Salvador L T, 2015. Shear resistance of bentonite backfill materials and their interfaces under varying hydraulic conditions in a deep rock nuclear waste repository. Applied Clay Science 104, 211–220.

Åkesson M, Kristensson O, Börgesson L, Dueck A, Hernelind J, 2010. THM modeling of buffer, backfill and other system components. Critical processes and scenarios. SKB TR-10-11, Svensk Kärnbränslehantering AB.

Appendix 1

Definitions and abbreviations

Abaqus	Commercial Finite Element software for multi-purpose numerical analysis.
Backfill	Backfill is the material or materials that is/are used for backfilling of deposition tunnels.
Boundary conditions	Nodal constraints in a numerical model (e.g. prescribed displacements on model sides).
Buffer	Compacted bentonite blocks and pellets surrounding the copper canister in the deposition hole.
Constitutive model	Conceptual model that simulates the stress-strain response of a material.
Contact surfaces	Surfaces separating regions of material where contact may or may not occur.
Deposition hole	The vertical hole where the disposal canister and the surrounding buffer are emplaced in the KBS-3V concept.
Deposition tunnel	The tunnel, where deposition holes are located in the KBS-3V concept.
Drucker-Prager failure envelope	Conical surface in the stress space, which defines the boundary between admissible and prohibited stress states.
Drucker-Prager model	Elastic-plastic constitutive model based on Drucker-Prager failure envelope.
Elastoplastic behaviour	Stress-strain relationship with updated stiffness depending on plastic strains (a.k.a. hardening plasticity).
Element mesh	Domain discretization for Finite Element analysis.
Failure envelope	Surface defining the boundary between admissible and not admissible stress states in a material.
Failure criterion	Equation defining failure condition based on a given failure envelope.
Finite Element code	Piece of software that calculates stress and strain distribution within a domain in accordance with external loads and boundary conditions where the material response is modelled through constitutive models.
Global load displacement curve	In the Buffer swelling test, the relationship between applied load and vertical displacement measured at the top of loading plate.
Hardening soil model	Constitutive model for loose soils suitable for sands and clays.
Hoek-Brown failure envelope	Failure envelope introduced by Hoek-Brown for rock based on semi-empirical approach.
Interface elements	Finite elements defining the behaviour at the contact between different material regions.
KBS-3V	(Kärnbränslesäkerhet 3-Vertikal). The reference design alternative of the KBS-3 method in which the spent nuclear fuel canisters are emplaced in individual vertical deposition holes.
Material Model	See Constitutive model.

Major principal stress	The greatest value of normal stress in a material.
ONKALO	The Olkiluoto Underground Rock Characterisation Facility.
OL1-4	Olkiluoto reactor units 1–4. OL1 and OL2 are BWR-reactors in operation, OL3 is EPR-type (in construction) and OL4 is so far only a decision-in-principle.
PLAXIS	Commercial Finite Element software for numerical analysis of geotechnical problems.
Performance target	*Safety functions* are the main roles for each barrier in establishing the long-term safety of the repository system, from which *performance targets* for the engineered barriers (canister, buffer, backfill, closure) and *target properties* for the host rock are defined considering their respective safety functions.
Reference case	Geometry and properties as assumed in buffer/backfill design.
Relative shear stress	Ratio between the mobilized shear stress and the maximum value the material is able to withstand according to a given failure envelope.
Repository	Part of the disposal facility consisting of deposition tunnels and holes.
Sensitivity analysis	(in numerical simulation) Study on the influence of the uncertainty of input variables on the final results.
Strength parameters	Parameter that defines failure condition according to a given failure envelope .
STUK	Radiation and Nuclear Safety Authority in Finland.
Uniaxial compression strength	The strength of a rock or soil sample when loaded at constant rate of deformation in one direction without lateral restraint.
VAHA	Posiva's requirement management system (in Finnish "Vaatimusten hallintajärjestelmä".
XRF	X-ray fluorescence, an analytical method used to determine the chemical composition of the material.
YJH-2012 programme	YJH refers to the Finnish word "ydinjätehuolto" meaning nuclear waste management. The YJH-2012 programme describes Posiva's plans for further research, development and design during 2013–2018.
Buffer swelling test	A field test performed in Äspö HRL used for simulating the swelling of buffer into dry backfill.
Äspö HRL	The Äspö Hard Rock Laboratory, Sweden.

Arkitektkopia AB, Bromma, 2018

SKB is responsible for managing spent nuclear fuel and radioactive waste produced by the Swedish nuclear power plants such that man and the environment are protected in the near and distant future.

skb.se